IEEE Access
Multidisciplinary | Rapid Review | Open Access Journal

Received 23 June 2023, accepted 12 July 2023, date of publication 18 July 2023, date of current version 26 September 2023.

Digital Object Identifier 10.1109/ACCESS.2023.3296589

RESEARCH ARTICLE

Multi-Objective Optimization of an Islanded Green Energy System Utilizing Sophisticated Hybrid Metaheuristic Approach

AYKUT FATİH GÜVEN[1], NURAN YÖRÜKEREN[2], ELSAYED TAG-ELDIN[3], AND MOHAMED MAHMOUD SAMY[4]

[1]Faculty of Engineering, Yalova University, 77200 Yalova, Turkey
[2]Faculty of Engineering, Kocaeli University, 41001 Kocaeli, Turkey
[3]Faculty of Engineering and Technology, Future University in Egypt, New Cairo 11835, Egypt
[4]Faculty of Engineering, Beni-Suef University, Beni Suef 62511, Egypt

Corresponding author: Mohamed Mahmoud Samy (Mohamed.samy@eng.bsu.edu.eg)

ABSTRACT Responding to the global call for sustainable renewable energy sources amidst growing energy demands, exhaustion of fossil fuels, and increasing greenhouse gas emissions, this study introduces a multi-objective optimization of an islanded green energy system. The focus is on the implementation of a sophisticated hybrid metaheuristic approach in a Hybrid Renewable Energy System (HRES) specifically designed for a university campus in Turkey. The developed HRES combines an array of technologies, including Photovoltaic (PV) panels, wind turbines, batteries, diesel generators, and inverters. One of the novel aspects of our work is the deployment of a rule-based Energy Management Scheme for effectively orchestrating the power flow between different system components. We employed various algorithms, namely Genetic Algorithm (GA), Firefly Algorithm (FA), Particle Swarm Optimization (PSO), and a novel hybrid of the Firefly and PSO algorithms (HFAPSO) to ensure optimal sizing of HRES. This proves critical for achieving a cost-effective system that can meet specific load demands and adhere to techno-economic indicators. Our study employed four distinct scenarios, with the optimal scenario being met through PV/Battery components. Our approach effectively addressed the high Total Gas Emissions (TGE) observed in scenarios 3 and 4, leading to uninterrupted annual load coverage with zero TGE and 100% renewable energy, akin to scenario 1. The simulation results demonstrate the supremacy of the HFAPSO algorithm in sizing HRES. This approach proved more effective than the HOMERPPro software tool, as well as the GA, FA, and PSO algorithms. In addition, a comparative analysis of the time performances of these algorithms highlighted the superior performance and convergence of HFAPSO. The application of the HFAPSO algorithm in the most efficient system configuration resulted in 2787.341 kW PV and 3153.940 kW Battery. This led to an annual system cost (ACS) of $479340.57, a net present cost (NPC) of $7777668.32, and an energy cost of $0.2201 per kWh. The system, entirely covered by solar panels, achieved a Renewable Energy Fraction (REF) of 100%.This study highlights the potential of efficient utilization and management of renewable energy sources through multi-objective optimization. Our method provides a valuable solution for reliably meeting energy demands and minimizing the annual cost of energy systems. The optimization was programmed using the MATLAB simulation package.

INDEX TERMS Energy management, microgrid sizing, hybrid energy system, hybrid firefly particle swarm optimization algorithms, renewable energy, techno economic optimization.

ACRONYMS AND NOMENCLATURE

ACS	Annual cost of the system ($).
BS	Battery storage.

The associate editor coordinating the review of this manuscript and approving it for publication was Behnam Mohammadi-Ivatloo.

COE	Cost of energy($/kWh).
CRF	Capital recovery factor.
CC	Cycle charging.
DG	Diesel generator.
DOD	Depth of discharge (%).
EMS	Energy management system.
GA	Genetic algorithm.
GWO	Gray wolf optimization.
GSA	Gravity search algorithm.
HFAPSO	Hybrid firefly particle swarm optimization.
FA	Firefly algorithm.
HRES	Hybrid renewable energy systems.
LCOE	Levelized cost of energy($/kWh).
LPSP	Loss of power supply probability (%).
LF	Load following.
NPC	Net present cost ($).
PV	Photovoltaics.
RES	Renewable energy sources.
PSO	Particle swarm optimization.
RE	Renewable energy.
REF	Renewable fraction (%).
SOC	State of charge value (%).
SOC_{max}	State of charge (max value) (%).
SOC_{min}	State of charge (min value) (%).
WT	Wind turbine.
Symbols	
$P_{WT}(t)$	Output power of WTs at time t (kW).
$P_{PV}(t)$	Output power of PVs at time t (kW).
$P_L(t)$	Load energy demand (kW).
$P_{Ren}(t)$	The total energy from renewable sources (kW).
$P_{ch}(t)$	Power available for battery charging (kW).
$E_{ch}(t)$	Energy charged to the battery (kWh).
$P_{distch}(t)$	Discharge battery power (kW).
$E_{distch}(t)$	Energy is discharged from the battery (kWh).
$E_{BS_{min}}$	Minimum battery energy (kWh).
$E_{BS_{max}}$	Maximum battery energy (kWh).
$E_{BS}(t)$	Energy of battery (kWh).
$E_{dump}(t)$	Energy dumped/wasted (kWh).
$E_{WT}(t)$	Energy of wind turbine (kWh).
$E_{PV}(t)$	Energy of photovoltaic panel (kWh).
$DG\_hr(t)$	Diesel generator is running at time t.
DG_P	The power produced by diesel generator. (kW)
O&M	Operation and maintenance($).
t	Time.
Greek symbol	
σ	The self-discharge rate of the battery.
η_{BD}	Battery discharging efficiency (%).
η_{BC}	Battery charging efficiency (%).
η_{Inv}	The efficiency of an inverter (%).

I. INTRODUCTION

In the world that has changed rapidly in the last decade, population growth and developments in digital technology, especially in developing countries, rapidly increase the electricity demand. Today, energy production is mainly relying on fossil fuels with finite resources such as natural gas, coal, and oil. Fossil fuels are an unsustainable source of emissions by greenhouse gasses that have negative effects on the ecosystem. Therefore, the popularity of renewable energy sources (RES) is increasing today [1].

Wind and solar energy systems are fast-growing, green, and renewable thanks to their low-cost construction. In addition, since they are sustainable and environmentally friendly domestic resources, they are also very important in terms of reducing external dependence [2].

Studies confirm that Turkey has a great potential for electricity generation using wind and solar energy. Unlike traditional energy sources, a renewable energy source is generally unstable and volatile [3]. In terms of solar and wind energy sources, the values of meteorological conditions and air velocity can vary greatly depending on the hour or day. This shift introduces a hard-to-estimate unpredictability that causes problems in regard to the reliability and stability of an energy system. There are unknowns caused by the variable properties of these green sources of energy, and these necessitate the use of storage (i.e., batteries) and backups (e.g., generators work on fuel). We, however, can mitigate these uncertainties through evaluating quantitative information of these renewable sources of energy, as well as planning appropriately, and optimizing and efficiently managing the systems of production. The fundamental and primary answer to these complexities is to use multiple renewable energy sources, which are called Hybrid Renewable Energy System (HRES). Within such a system, an increase in the quantity of energy sources allows for lower-cost energy production than a single renewable energy source for the hours and seasons needed. However, because of the variable properties of energy sources, the difficulty in calculating an effective cost estimate, and the lengthy in-process processes of the optimizers used in ideal sizing, recalibrating the most suitable shape and size for the load demand in a particular region is often difficult [4].

In the literature screening on hybrid renewable energy systems, various studies focusing on various properties of such systems have been found. Out of these, power management of HRESs and optimization methods for sizing draw attention. Various components are combined and used along with each other to create a hybrid system in renewable energy systems with grid-connected or off-grid structures. In hybrid systems, the power management and the size of each component should be optimally adjusted to ensure the system's cost-effectiveness and reliability [5]. Wind/solar/battery/diesel generator renewable energy components can be combined in various ways.

HOMERPro software has been used in several studies to determine the best operating parameters for systems that are grid-connected and/or off-grid, based on PV, Wind Turbine (WT), Diesel Generator (DG), and Battery (BS) elements [6], [7], [8], [9], [10]. In addition, optimization studies are using traditional and metaheuristic algorithms. For similar systems, Das et al. optimized the HRES for an island community in Bangladesh to provide reliable electricity services along with fresh water, and this HRES was not shared by the national grid. Genetic Algorithm (GA), Particle Swarm Optimization (PSO), as well as a hybrid of them were used in the optimization process [11]. In the study by Mokhtara et al., HRES with PV/WT/DG/BS components was conceptualized in an optimal setting for rural dwellings. The PSO algorithm was used to investigate the effect of the structure's climate variability and energy efficiency on the optimal HRES sizing [12]. In the study by Dehaj et al., an HRES was modeled and optimized for different wind, sun, and ambient temperature conditions of various cities in Iran. The two chosen simultaneous objective functions were total annual cost and fuel ratio. PSO was used to determine the optimal value for the design parameter [13].

Zhu and colleagues developed an island-based HRES, composed of tidal current and wind turbines along with battery storage systems. This system was specifically designed for autonomous marine applications, taking into account the essential factors of climate resources and valuable land resources. To minimize the probability of power supply loss, energy discharge probability, and energy costs, a revised version of the multi-objective Gray Wolf Optimizer (GWO) has been proposed, grounded on the Halton sequence and social motivation strategy [14]. Javed et al. conceptualized hybrid solar-wind energy system optimization with storage, with a mathematical model using the GA. The analysis spanned across four different states, and the results were compared using the commonly utilized HOMERPro software. The comparison revealed that the Genetic Algorithm (GA) method could deliver a more optimal system concerning reliability and cost-effectiveness than HOMERPro [15]. In the context of a rural location within Namibia's Namib Desert, Chen and his team have proposed an optimal hybrid system dedicated to meeting energy load demands. To ensure minimum levels of CO2 emissions, annual costs, and the potential for system loss, an ε-constraint technique was employed alongside an enhanced Crow Search Algorithm. The effectiveness of the proposed algorithm was later validated. The optimization of the system was compared with both HOMERPro and methods based on PSO, underlining the efficiency of the proposed method [16]. Saraswat and Suhag, focusing on a community in Kurukshetra, India, conducted an investigation into the optimal economic sizing of an autonomous HRES, consisting of PV/WT/DG/BS components. It was found that the Whale Optimization Algorithm provided a solution that was superior in terms of Levelized Cost of Energy (LCOE), Net Present Cost (NPC), and payback time when compared to solutions offered by the PSO, Gravity Search Algorithm (GSA), GWO, and hybrid PSO-GSA algorithms [17]. Elsewhere, Das and his colleagues concentrated on assessing the technical, economic, and environmental facets of hybrid renewable energy systems on an isolated island in Bangladesh. They engineered a hybrid energy system, which amalgamated several renewable energy sources, including wind, solar, and hydraulic power, using a multi-objective genetic algorithm. Subsequently, the team analyzed the technical, economic, and environmental performance of this system [18]. In addition to these studies, a variety of methodological approaches have been proposed to enhance the optimization of hybrid energy systems. For instance, Liu and his team introduced a deep learning-based optimization strategy aimed at managing home energy. This innovative approach aids homeowners in reducing their energy bills by optimizing their home energy consumption through the use of deep learning algorithms [19]. Foruzan and his colleagues, on the other hand, suggested a power learning approach aimed at achieving optimal distributed energy management in a microgrid. The goal of this approach is to reduce energy costs while enhancing system stability [20]. Morteza and his colleagues introduced a deep learning framework to evaluate the flexibility of energy transmission lines. The objective was to gather more information on the flexibility of the energy transmission infrastructure to devise more effective energy management strategies [21]. In another study, a deep learning-based predictive model was utilized for energy management within a microgrid, and a predictive energy management strategy was proposed. This novel approach utilized deep learning algorithms to anticipate energy consumption, providing a more in-depth understanding of the grid's energy needs [22]. The considerable extent of research underscores the vital role of renewable energy systems in considerably curbing greenhouse gas emissions, thus aiding in achieving global sustainability objectives. One such study by Ahmet et al. underscores the critical role of hybrid renewable energy systems in significantly mitigating carbon emissions, setting a course towards a greener and more sustainable future [23]. Furthermore, an extensive exploration by Lu et al. highlights the benefits of deploying a sophisticated hybrid metaheuristic approach in energy systems, leading to an optimized and more energy-efficient system and an overall decrease in emissions [24]. Moreover, Ahmed et al. have examined the influence of environmental initiatives in promoting corporate entrepreneurship and green innovation [25]. They stress the crucial role of green value co-creation as a mediator. Similarly, Alvi et al. have conducted a comprehensive analysis of photovoltaic power systems from technological, financial, and ecological perspectives, using the RETScreen® tool in a case study in Khuzdar, Pakistan [26]. This research exemplifies the practical use of RETScreen® in renewable energy ventures. Mirzahosseini and Taheri, meanwhile, have carried out a feasibility study of solar power plants from environmental, technical, and financial angles using RETScreen,

demonstrating how economic and policy elements overlap with the implementation of renewable energy in Iran [27]. In another vein, Psomopoulos et al. offered a comparative analysis of various software for assessing photovoltaic electricity production, emphasizing the importance of suitable tool selection for energy project evaluation [28]. Ahmed et al. and Basu have significantly contributed to the evolution of optimization methods for power dispatch issues [29], [30], [31], [32]. These investigations have unveiled various facets of multi-area economic emission dispatch for large-scale, multi-fueled power plants, contemplating interconnected grid tie-lines power flow limitations, and multi-county combined heat and power dynamic economic emission dispatch incorporating an electric vehicle parking lot. Ahmed et al.'s work on a dynamic optimal scheduling strategy for multi-charging scenarios of plug-in electric vehicles over a smart grid provides novel insights into managing EV charging within the framework of smart grids [33].

Building upon these and other studies, researchers have traditionally turned to conventional and metaheuristic optimization techniques for performance analysis within software tools. Yet, these tools exhibit substantial limitations, including a higher demand for core hours compared to existing optimization techniques. A wide body of research on hybrid systems proposes a range of traditional and evolutionary algorithms for determining optimal component sizing. A myriad of metaheuristic evolutionary algorithms have been developed to tackle the pervasive problem of traditional techniques falling into local minima, particularly in grid-independent frameworks using PV/WT/DG/BS components [34].

In contrast, this study aims to design an optimized HRES that provides reliability, cost-effectiveness, and reduced pollution for a selected area. To accomplish this, the study employs meteorological parameters to estimate the power output of wind turbines and PV panels. The study minimizes the Annual Cost System (ACS) value of the HRES using various methods, including PSO, GA, Firefly Algorithm (FA), and Hybrid Firefly Particle Swarm Optimization (HFAPSO). The optimal dimensions of the system's components are determined through a comparative analysis of the results of each algorithm using multiple metaheuristics. The HFAPSO algorithm proved particularly efficient in tackling the HRES sizing issue, showing superior speed compared to other commonly used algorithms and the HOMERPro software. This study addresses a problem set intrinsic to HRES. These systems exhibit a high degree of complexity due to factors such as the expansion of the search space, the presence of intricate constraints, the inherent variability of renewable energy sources, and challenges related to energy storage system sizing and the harmonious operation of diverse energy production sources. Traditional mathematical optimization techniques are found to be inadequate in this scenario, leading to the adoption of the HFAPSO algorithm for this study. This hybrid algorithm demonstrates its robustness in achieving the global optimum solution and managing the complex constraints associated with HRES. The amalgamation of FA and PSO techniques contributes to a comprehensive and efficient search space, thereby presenting a significant advantage in the problem-solving process.

This paper is structured into five sections. Chapter 2 describes the modeling of the hybrid energy system and its renewable energy components. Chapter 3 outlines the methodology, including system modeling, energy management strategy, load demand, optimization algorithms, and process. Chapter 4 presents the simulation results and discussions for the HRES.

II. MATERIAL AND METOD

This section provides a detailed description of the hybrid energy system modeling, including the specifics and mathematical modeling of the components. It delves into the evaluation of renewable energy sources, load demand, and economic calculations, as well as cost optimization and techno-economic constraints. The techniques used in the optimization process and the execution steps are also discussed. The primary objective is to meet the electrical load demand at the lowest possible cost by employing the most efficient design of an off-grid hybrid energy system. In this study, the micro energy system is optimized using the Hybrid Optimization of Multiple Energy Resources (HOMER) software, in conjunction with four different metaheuristic algorithms. Figure 1 presents a block diagram illustrating the research methodology.

A. MODELING OF HYBRID RENEWABLE ENERGY

The standalone microgrid outlined in this paper is built using wind turbines, battery components, diesel generators, and solar panels. Figure 2 shows a schematic of the planned standalone hybrid PV/WT/BS/DG energy system. Before determining the optimal size of the HRES, modeling of system components is a prerequisite. Consequently, a thorough model of the system's parts is provided below.

B. MODELING OF PHOTOVOLTAIC SYSTEM

Photovoltaic panel power generation refers to conversion of sun light to electricity. The PV system is assumed to have Maximum Power Point Tracker (MPPT), so that highly efficient maximum power is obtained from PV system. In this study, a simplified model that consider solar irradiance and ambient temperature is used, as shown in the following Equation (1) [35].

$$P_{pvout}(t) = P_{PV_{rated}} \times \frac{G(t)}{1000} \times \left[1 + \alpha_t \left((T_{amb} + (0.0256 \times G_t))\right) - T_{ref}\right] \quad (1)$$

Here, $P_{pv_{out}}(t)$ represents the PV module output power (W), $G_{(t)}$ represents the value of solar radiation (W/m2), $P_{(PV_{rated})}$ represents nominal PV power under standard conditions, α_t represents the coefficient of temperature calculated by $(-3.7 \times 10^{-3}$ (1/°C)), $T_{ref} = 25$°C is the reference temperature under standard conditions, T_{amb} is the ambient temperature (°C).

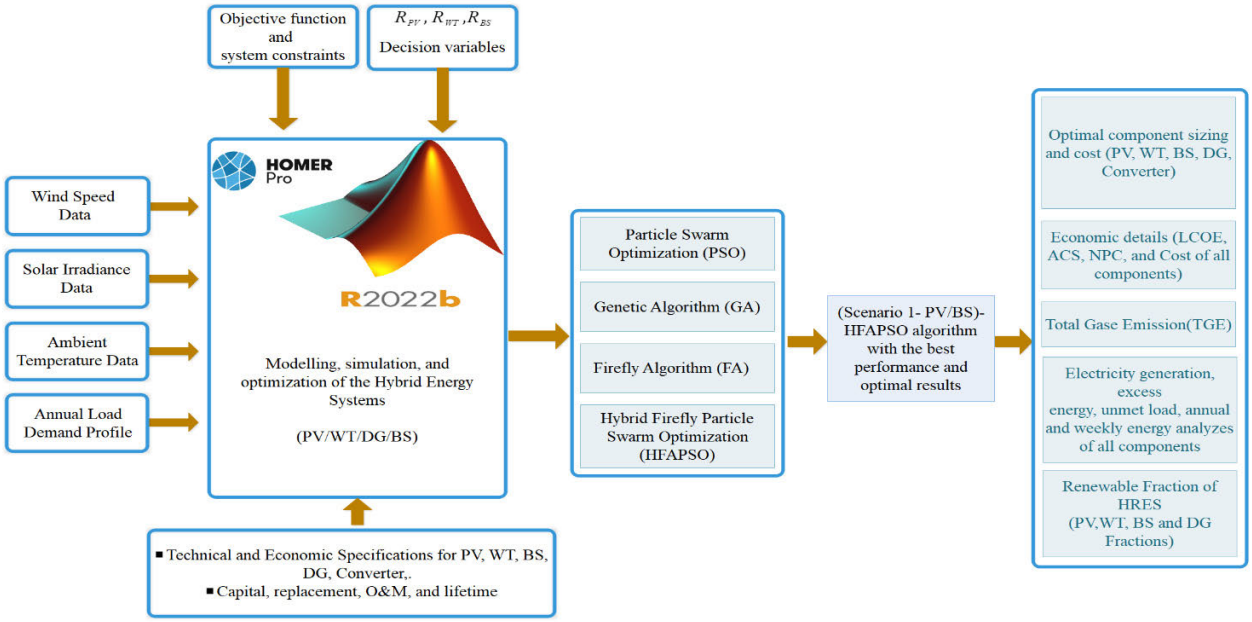

FIGURE 1. HRES optimization methodology flowchart.

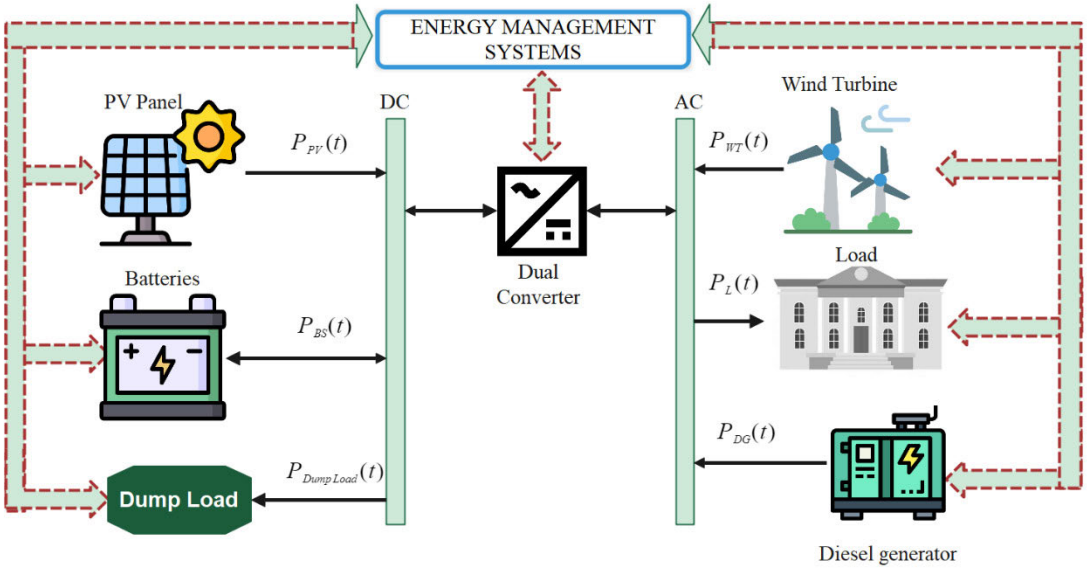

FIGURE 2. Standalone hybrid renewable energy system.

C. MODELING OF WIND TURBİNE

The best model should be used to calculate the output power of a wind turbine. The Equation (2) is often used to calculate the power output of a wind turbine [36]. In meteorological stations, the normal height for measuring wind speed with an anemometer is 10 m.

$$P_{WT} = \begin{cases} 0 & v(t) \le v_{cut-in} or v(t) \ge v_{cut-out} \\ P_r \times \dfrac{v(t) - v_{cut-in}}{v_r - v_{cut-in}} & v_{cut-in} \le v(t) \le v_r \\ P_r & v_r \le v(t) \le v_{cut-out} \end{cases} \quad (2)$$

Here, the following are the corresponding parameters of the wind turbine: P_r (kW) is the nominal power, and the speed parameters for the following are as follows: $v(t)$ (m/s): wind, $v_{cut-out}$ (m/s): cut-out, v_r (m/s): nominal, and v_{cut-in} (m/s): cut-in.

Since wind speed is usually measured at a certain position, wind speeds at higher or lower locations can be predicted using the power exponent (a_h) in Equation (3).

$$V_t = V_m * \left(\frac{H_t}{H_m}\right)^{a_h} \quad (3)$$

In Equation (3), the following are the corresponding parameters of the wind turbine: H_t represents the wind turbine hub height, H_m represents the reference height, V_m (m/s) represents the reference wind speed measured at H_m, V_t (m/s) represents the wind speed measured at the hub's level H_t, while a_h represents exponential power law's value. The exponent a_h depends on the topography and site climatic conditions. The numerical value of a_h depends on the surface roughness and environmental stability, and falls between 0.05 and 0.5. a_h is assumed to be 0.14 in the chosen locations.

D. MODELING OF BATTERY

It is critical to accurately model the battery to keep up with the load demand, especially when you consider that the procedure of battery storage is stochastic given the nature of the outputs of PV cells and WTs. The batteries are charged when the energy generated by renewable energy resources exceeds the total load demand. However, when the load demand exceeds the generated power, the batteries are discharged to close the energy gap. Equations (4) and (5) are used to evaluate the charging and discharging processes of the batteries, respectively [37].

$$E_{ch}(t) = E_{BS}(t-1) \times (1-\sigma) + \left[\left(E_{WT}(t)/\eta_{Inv}\right) + E_{PV}(t) - \frac{E_{Load}(t)}{\eta_{Inv}} \right] \times \eta_{BC,} \text{Charging mode} \quad (4)$$

In the opposite case, that is, when the load demand is not met by the total power produced by various sources, the battery storage bank will take the control and supply the needed energy, and thus the battery storage bank starts to be discharged. As a result, Equation (5) shown below can be used to represent the available battery storage bank capacity at hour 1 of the discharge.

$$E_{dch}(t) = E_{BS}(t-1) \times (1-\sigma) + \left[\frac{E_{Load}(t)}{\eta_{Inv}} - \left(\left(E_{WT}(t)/\eta_{Inv}\right) + E_{PV}(t)\right) \right] \times \eta_{BD,} \text{ Discharging mode} \quad (5)$$

Here, E_{BS} (t) is the energy stored in battery at hour t (kWh), E_{BS} (t − 1) is the energy stored in battery at hour (t-1) (kWh), σ represents the battery storage bank rate of self-discharge, E_{PV} represents the energy production of the PV-module at hour t (kWh), E_{WT} represents the energy production of the wind turbine at hour t (kWh), E_L stands for the load demand at hour t (kWh), η_{BC} is the battery charging efficiency, η_{BD} is the battery discharging efficiency, and η_{Inv} represents the efficiency of the inverter. The η_{BC} and η_{BD} values given above, will vary depending on the charging current at each stage. For the purposes of this study, the charging efficiency was considered to be constant at 90%.

When renewable energy sources generate a surplus of power, it is stored in battery banks. However, Battery capacity should be limited. The battery storage bank is incapable of storing large amounts of energy. The maximum allowable depth of discharge (DOD) is displayed in percentages. It is not possible to discharge a battery completely. In this study, it was assumed to be 80%. Equation (6) was used to calculate the minimum battery storage capacity [38].

$$E_{BSmin} = (1 - DOD) \times E_{BSmax} \quad (6)$$

Additionally, the battery bank capacity restriction at any hour was expressed by Equation (7). The dump load will draw excess energy produced by the renewable energy sources but unused when the load does not need all the energy and the battery bank storage has reached its maximum capacity and cannot store more energy.

$$E_{BSmin} \le E_{BS}(t) \le E_{BSmax} \quad (7)$$

In the equations, the maximum acceptable battery discharge as a percentage is represented by DOD, and E_{BSmax} and E_{BSmin} are the max. and min. permissible storage capacity, respectively.

E. MODELING OF DIESEL GENERATOR

A diesel generator compensates for the absence of adequate power output by the resources such as PV or Wind and a battery bank in a hybrid system. A diesel generator adds reliability in a hybrid system. Regular repair and maintenance is always recommended to enhance the life span of the generator. The fuel spent by a diesel generator is defined by Equation (8) and is entirely predicated on the power output of the generator.

$$F(t) = a_{dg} \times P_{DG}(t) + b_{dg} \times P_r \quad (8)$$

Here, the following are the corresponding parameters of DG are as follows: $P_{DG}(t)$ represents the generation of power at hour t (kW), F(t) represents the consumption of fuel (L/h), P_r represents the average power, while a_{dg} and b_{dg} (L/kW) represent values that are constants and symbolize the standardized parameters for fuel consumption, that are 0.246 and 0.08415, respectively [39].

F. MODELING OF INVERTER

For any hybrid energy system to function properly, it is common that one or more power converter to be incorporated into the system. Inverters are pieces of electronic equipment that convert direct current to alternating current. Here converter is used which can work both as an inverter and rectifier depending on the direction of flow of power. Equation (9) can be used to calculate the inverter's input power (P_{inv}) [39].

$$P_{inv}(t) = P_L^{max}(t)/\eta_{inv} \quad (9)$$

Here, $P_L^{max}(t)$ represent the peak power demand which is the maximum power required by the load at time t. η_{inv} represents the efficiency of the invert. Data regarding the inverter are presented in Table 1.

TABLE 1. Economical and technical parameters of microgrid components.

Description		Parameter	Value	Unit
A.	Photovoltaic Panel	Solar panel-rated capacity	0.345	kW
		Solar panel temperature coefficient	-0.390	
		Operating temperature	44	^{0}C
		Efficiency	17.8	%
		Panel lifespan	20	Year
		Capital cost of PV	650	$/kW
		Replacement cost of PV	650	$/kW
		Maintenance and Operation cost	50	$/year
B.	Wind Turbine	Turbine rated power	1	kW
		Hub height	17	m
		Installation cost	2000	$/kW
		Replacement cost	2000	$/kW
		Maintenance and Operation cost	200	$/year
		lifespan	20	Year
C.	Battery Storage Bank	Rated voltage	600	V
		Rated capacity	100	kWh
		Capacity(max)	167	Ah
		Round-trip efficiency	90	%
		Battery charging current (max)	167	A
		Battery charge status (min)	20	%
		Discharge current (max)	500	A
		Lifespan	10	Year
		Capital cost	550.00	$/kW
		Replacement cost	550.00	$/kW
D.	Diesel Generator	Capacity	1000	kW
		Replacement cost	175	$/kW
		O&M cost	30	$/kWh
		Capital cost	175	$/kW
		Fuel price	1	$/L
		Lifespan	10	Year
E.	İnverter	Capacity	1	kW
		O&M cost	50	$/year
		Capital cost	300	$/kW
		Replacement cost	300	$/kW
		Efficiency	95	%
		Lifespan	15	Year
F.	Economic Parameters	Rate of interest in Turkey	19	%
		Rate of inflation in Turkey	16.59	%
		Rate of discount in Turkey	8	%
		lifespan	20	Year

G. DATA ON THE ECONOMIC PARAMETERS OF THE ENERGY SYSTEM

The impact of sensitive variables affecting the feasibility of a hybrid-energy system should be considered for financial analysis. The working economic parameters in the study were set at a 19% real interest rate, a 16.59% inflation rate, and a 8% discount rate. The hybrid energy system is expected to last 20 years. The manufacturers provided the actual cost pricing of the HRES components, which were used in the simulations. Table 1 shows the specifications for the economic and technical facets of the microgrid elements.

H. LOAD ASSESSMENT OF THE STUDY AREA

The research site for the study is the university campus, situated at latitude 40°39.2'N and longitude 29°13.2'E. The General Directorate of State Meteorology provided meteorological data for the study area for 2022, and wind speed (per hour), solar radiation, the temperature of the ambient, and load curves were drawn for the entire year. The maximum load per hour at the university was approximately 1007.6 kW/year, while the minimum demand was 248.59 kW/year. The average daily consumption of electricity was 5966.00 kWh. Figure 3 depicts the load profile for a one-year cycle in the chosen case study (8760 hours). Actual load values for the study region were used in this research.

I. CLIMATE DATA

The suggested HRES's sizing optimization problem was solved using HOMERPro and MATLAB tools, which also helped to identify the best configurations for the chosen location. Many applications use MATLAB software to solve multi-objective optimization problems in hybrid energy sytem using a variety of strategies and algorithms. Before beginning the calculation, MATLAB needs the load profile for the chosen location, the economic and technical parameters of the hybrid energy system components, and the hourly time step of the region climate data. The hourly profiles of wind speed, solar radiation, and ambient temperature over a year are depicted in Figures 4, 5, and 6, respectively.

III. METODOLOGY

This chapter describes the methods used to find answers to the study's research questions. The subsections explain the HRES sizing, strategy for energy management, objective function, as well as optimization algorithms utilized in the methodology.

In this work, a renewable standalone solar panel/wind turbine HRES employing battery banks and diesel generator unit is optimized first with the help of HFAPSO Algorithm considering the ACS analysis. Size optimization of the above hybrid energy system is the main objective of the work. The site of the hybrid system is situated at Turkey. Solar and wind are the main renewable sources in the system and batteries and diesel generator unit or are the supplementary

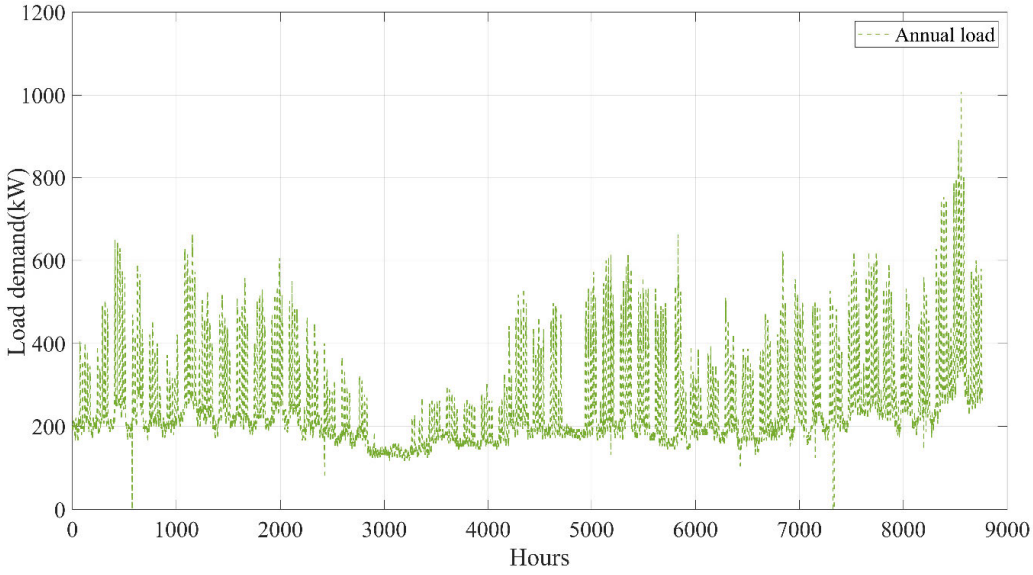

FIGURE 3. Annual load profile for the campus.

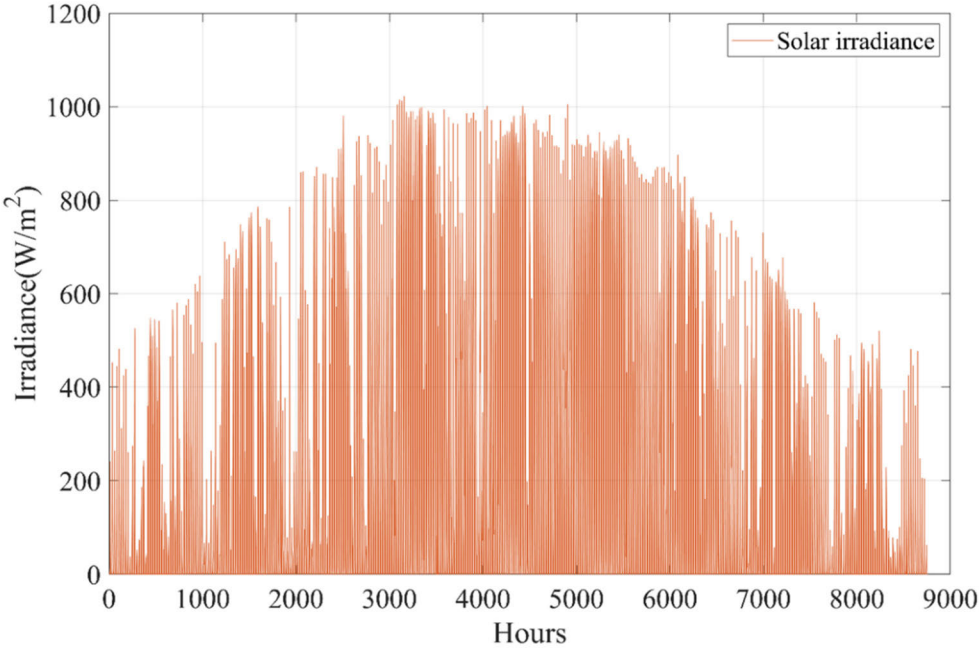

FIGURE 4. Solar radiation data(W/m2).

sources. System modelling is the most important part of any optimal sizing process. The different component model, like PV module, wind turbine model, battery model and generator model, is described in the earlier chapter. Power equations are used as a function, which will give power output depending on different values of solar irradiance and wind speed. The produced power from the different models is used in system simulation. Depending on the value of produced primary energy (solar and wind power), the battery bank and the diesel generator unit will operate.

A. ENERGY MANAGEMENT STRATEGY (EMS)

A robust EMS is a critical component that needs to be carefully planned during the process of planning microgrids. EMS manages the power flow between different components [40], and while reducing degradation of the battery, it maximizes Renewable energy system usage and minimizes the fuel consumption. Furthermore, system efficiency is improved, as a result, EMS provides valuable savings on the expenses on costs and energy. Focusing on a rule-based method, the EMS controller used within the current research was created with

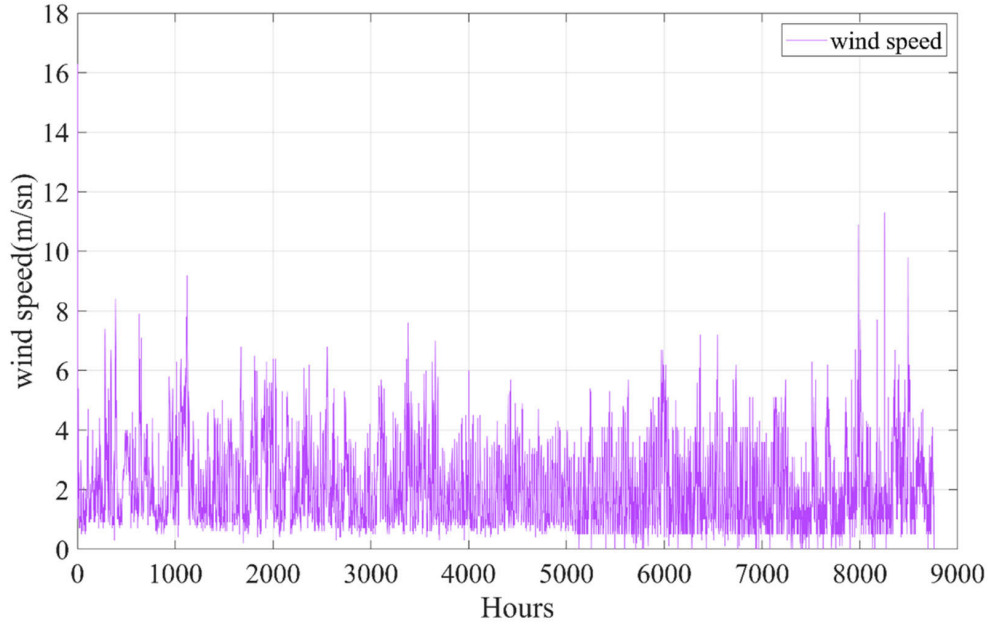

FIGURE 5. Wind speed data (m/s).

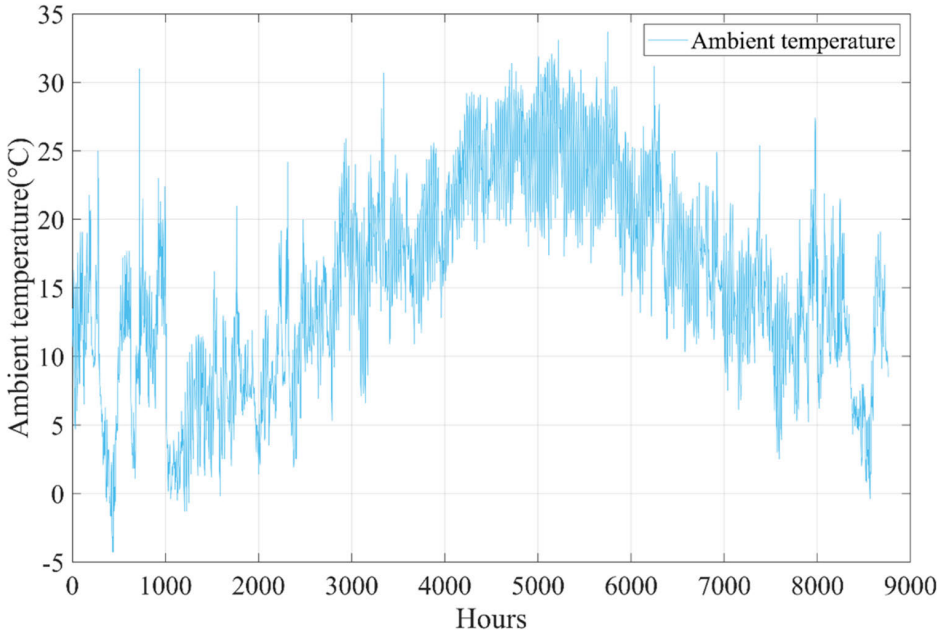

FIGURE 6. Ambient temperature data (C0).

"if, else, and then" commands. Because the EMS controller used the cycle charging approach, it functioned under the criteria mentioned below:

Case no.1: Renewable energy resources generate enough energy to meet the energy-load requirement. The surplus energy is set aside to charge the battery bank. (E_{BS} (t) < E_{BSSmax} (t))

Case no.2: Renewable energy resources generate more energy than the requirement. A dump load consumes the surplus. (E_{BS} (t) = E_{BSmax} (t))

Case no.3: Renewable energy resources generate insufficient energy to meet the demand. (E_{Batt} (t) > E_{Batt_min} (t)). The batter bank uses the stored energy to compensate.

Case no.4: Renewable energy resources generate insufficient energy to meet the demand; the battery is depleted (E_{BS} (t) < E_{BSmin} (t)). The DG is then run with the purpose of meeting the load demand, then the battery bank is recharged. The DG turns off the energy supply once the renewable energy resources have resumed power production.

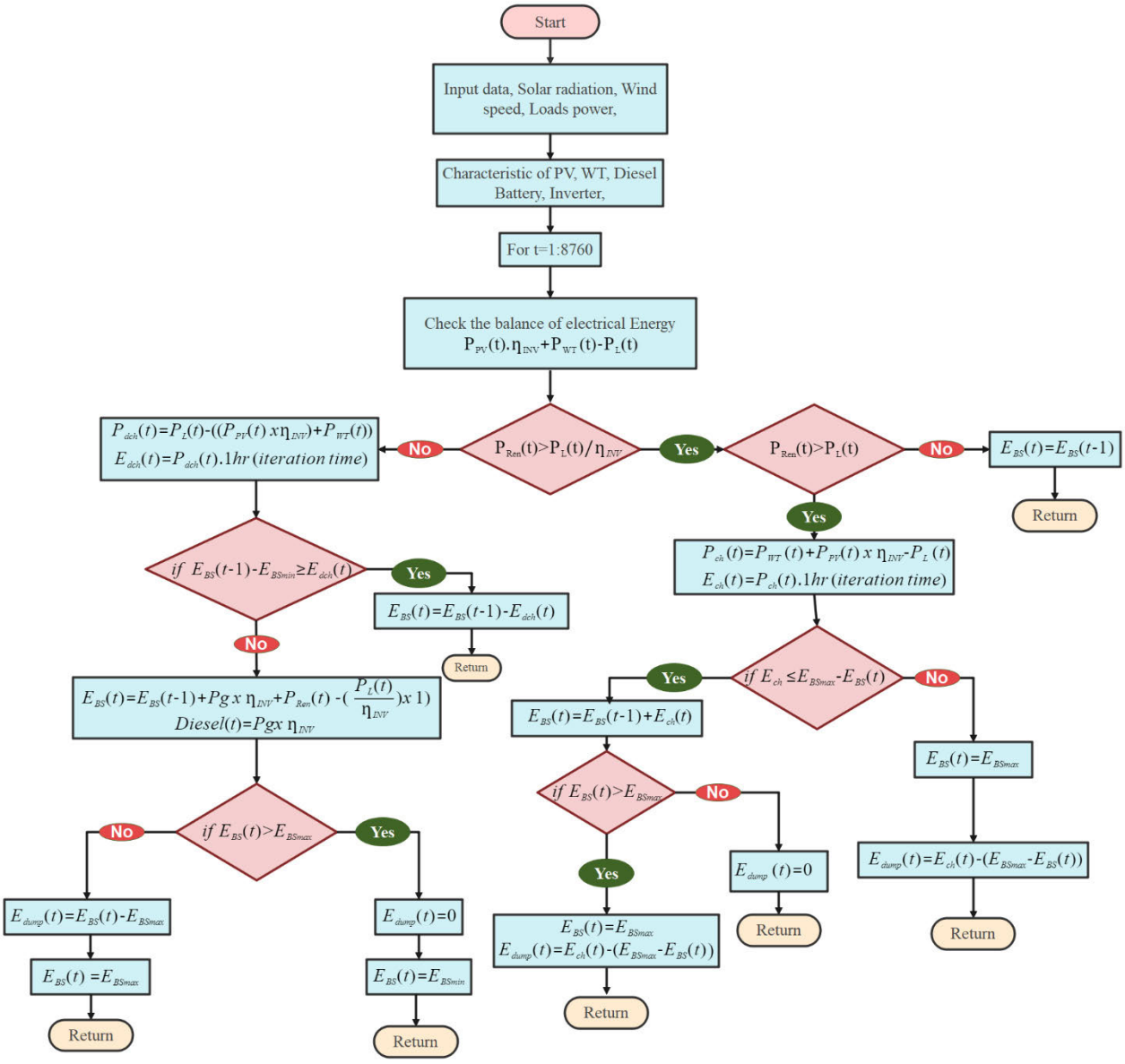

FIGURE 7. Chart of the operating strategy of the proposed hybrid energy system.

The flow algorithm of the specified hybrid-energy control framework is depicted in Figure 7. The diesel generator and battery bank are positioned in the organizational plan of this optimization technique as wind-based and solar elements' fail-safe. The operational strategy's marks such as load demand, solar energy, and wind energy are initially validated. The volume of renewable energy generated is weighed against the load demand.

B. OBJECTIVE FUNCTION OF HYBRID ENERGY SYSTEM

An economic analysis is required to determine the optimum cost and benefit ratio of HRES. These systems generally require high capital investment, even though they have low operation and maintenance costs and less fuel costs in comparison with systems relaying only on fossil fuels. In literature, many economic based sub-models to evaluate HRES can be found in. In this study, the ACS, NPC, and the LCOE are considered as the economic criteria to evaluate the feasibility of this hybridized system configuration. The three main decision factors for the optimal configuration are the number batteries, WT power, and PV power. According to all other parameters and constraints, the result with the value of lowest ACS, NPC, LCOE for the Techno-Economic analysis is optimal. Total capital and replacement costs, as well as cost of operation, and cost of maintenance comprise the objective function used here. Installation and construction costs are included in the component capital costs. ACS, LCOE, TNPC, PV, WT, DG, BS capacity, and inverter capacity are decision

variables. Equation (10) defines the objective function.

$$OF = Min(ACS, LCOE, NPC) \tag{10}$$

The LCOE is NPC-dependent, and it includes the costs of O&M and replacement [41]. Here, the PV, WT, BS, and DG component costs are taken into account. Below equations help calculate the LCOE to be minimized.

$$C_t^{PV} = N_{PV}\left(C_C^{PV} + C_{O\&M}^{PV} \times \left(\frac{(1+i)^n - 1}{i(1+i)^n}\right)\right) \tag{11}$$

$$C_t^{WT} = N_{WT}\left(C_C^{WT} + C_{O\&M}^{WT} \times \left(\frac{(1+i)^n - 1}{i(1+i)^n}\right)\right) \tag{12}$$

$$C_t^{BS} = C_C^{Batt} + C_{O\&M}^{BS} \times \left(\frac{(1+i)^n - 1}{i(1+i)^n}\right) C_R^{BS} \times \sum_{j=1}^{\left(\frac{n}{n_{Batt}}-1\right)} \left(1 + \frac{1}{(1+i)^{jn_{BS}}}\right) \tag{13}$$

$$C_t^{DG} = C_C^{DG} + C_{O\&M}^{DG} \times \left(\frac{(1+i)^n - 1}{i(1+i)^n}\right) + C_R^{DG} \times \sum_{j=1}^{\left(\frac{n}{n_{DG}}-1\right)} \left(1 + \frac{1}{(1+i)^{jn_{DG}}}\right) \tag{14}$$

Equation (15) written below is used to calculate NPC:

$$TNPC = C_t{}^{PV} + C_t^{WT} + C_t^{BS} + C_t^{DG} + C_C^{Inv} \tag{15}$$

Here, N_{PV} and N_{WT} respectively indicate the number of photovoltaic power systems and the number of wind turbine power systems. C_C^{PV}, C_C^{WT}, C_C^{BS}, C_C^{DG}, and C_C^{Inv} represent PV, WT, BS, DG, and investment costs of components of the inverter in that order. $C_{O\&M}^{PV}$, $C_{O\&M}^{WT}$, $C_{O\&M}^{BS}$ and $C_{O\&M}^{DG}$ are PV, WT, battery storage bank and diesel generator components' O&M costs. C_R^{BS} and C_R^{DG} represent the battery and diesel generator components' replacement costs. i represents the annual interest, n represents system's lifecycle, while n_{BS} and n_{DG} stands for the lifetime of the components of the battery and diesel generators.

LCOE is a well-known and widely used parameter for determining the economic viability of microgrid systems [42]. It is expressed in Equation (16).

$$LCOE(\$/kWh) = \frac{TNPC}{\sum_{t=1}^{8760} P_{load}(t)} \times CRF \tag{16}$$

P_{load} denotes the load's power consumption per hour. Equation (17) can be utilized to calculate the annual capital cost by dividing the initial cost by the annual capital cost. CRF stands for capital recovery factor.

$$CRF(i_r, n) = \frac{\left[i_r \times (1+i_r)^n\right]}{\left[(1+i_r)^n - 1\right]} \tag{17}$$

HRES's project life cycle is represented here by n (years), real interest (%), and i_r.

C. LOSS OF POWER SUPPLY PROBABILITY (LPSP)

When evaluating a microgrid setup's reliability, the LPSP value is often used. The probability of a power supply failure to satisfy the energy demand is indicated by the LPSP reliability index. The value of LPSP is calculated by the division of the total energy deficit in the system by the total load over the operational period (T), that is usually a year. Equation (18), as shown at the bottom of the next page, is used to measure LPSP [43]. where, P_{WT} (t) represents wind turbine's power output at time step t, P_{PV} (t) represents PV system's power output at time t, P_{DG} (t) represents diesel generator's power output at time step t, P_{load} (t) represents the power consumed at time step t, and E_{BSmin} (t) represents the battery storage system's minimum allowable storage capacity.

Moreover, the state depicted in Equation (19) is utilized in the reliability assessment.

$$P(t)_{load} > P(t)_{generation} \tag{19}$$

LPSP has a value between 0 and 1; here, 0 indicates a fulfilled energy demand, while 1 represents an unfulfilled energy demand [44]. In this case, the simulation is run with the LPSP value set to zero.

D. RENEWABLE ENERGY FACTOR (REF)

To assess the contribution of renewable energy sources to the hybrid system, a variety of indices are used. REF was chosen to reduce the use of nonrenewable energy sources. Equation (20) below can be used to calculate the REF value when HRES is a diesel generator.

$$REF\ (\%) = \left(1 - \frac{\sum_{t=1}^{8760} P_{DG}(t)}{\sum_{t=1}^{8760} P_{PV}\ (t) + P_{WT}\ (t)}\right) \times 100 \tag{20}$$

Here, $P_{DG}(t)$ represents the energy produced by the diesel generator, while $P_{PV}\ (t) + P_{WT}\ (t)$ represents the energy supplied to the load at time step t.

REF is maximized by minimizing the second side of the equation. This is a limited value that cannot exceed 100%. As a result, as shown in Equation (21), the REF should always be less than the desired value ε REF) during the optimization process [45].

$$REF\ (\%) \leq \varepsilon_{REF} \tag{21}$$

E. GREENHOUSE GASES EMISSION OPTIMIZATION MODEL

Greenhouse gas emissions (GHG) from a hybrid renewable energy system are an important factor to consider. The more greenhouse gases emitted by the system to be installed, the greater the environmental damage. The Diesel generator, which emits three different gases, is the main component of the system responsible for this gas emission. These gases are CO_2, SO_2 ve NO_x. The total gas emission (TGE) of the system is calculated using Equation (22):

The emission factors 697, 0.5, and 0.22 are used in the study for CO_2, SO_2 ve NO_x, respectively [34].

$$TGE = \sum_{t=1}^{8760} \left(\left(a_{CO_2} + a_{SO_2} + a_{NO_x}\right) \times P_{DG}(t)\right) \tag{22}$$

F. DUMP ENERGY EVALUATION

Another minimization target of algorithms used in the optimization process is Dump Energy. The discharge process occurs when there is an excess of renewable energy generation and the battery reaches its maximum state of charge, which is not desirable because it wastes energy. To avoid this, the unloading energy can be consumed by the unloading load, campus irrigation, pumping systems, and the use of a three-phase resistor. The discharge energy is minimized in this study by employing an efficient hybrid HFAPSO algorithm-based optimal system design. The total Dump energy over the system's life cycle is also calculated using Equation (23):

$$D_{total} = \sum_{t=1}^{8760} E_{WT}(t) + E_{PV}(t) - \frac{E_{Load}(t)}{\eta_{Inv}} \tag{23}$$

G. DESIGN VARIABLES

Equation (24) shows the decision variables' lower and upper bounds, that are established as solar panel power, wind turbine power, and number of batteries.

$$Decisonvariables = \begin{cases} 1kW \leq R_{WT} \leq 10000kW \\ 1\,kW \leq R_{PV} \leq 10000kW \\ 1 \leq R_{BS} \leq 5000 \end{cases} \tag{24}$$

Here, R_{WT} is the wind turbine power, R_{PV} is the solar panel power, and R_{BS} is the number of batteries. The determination of the boundary values of the optimization decision variables is largely problem-dependent due to the number of variables and the complexity of the search space. Although these values were determined by trial and error in general, limit values were revealed in this study's simulation using the HOMERPro software. As a result, the values in Equation (24) were used to allow the algorithms in the MATLAB environment to converge to the optimal solution as quickly as possible.

H. OPTIMIZATION TECHNIQUES

Each optimization algorithm carries distinct strengths and weaknesses within the complex realm of optimization. Appreciating these nuances and strategically implementing a hybrid approach could potentially provide a greater degree of robustness and flexibility. This attribute becomes especially beneficial when addressing multifaceted design problems.

In this section, our focus is on a hybrid algorithm initially proposed by Aydilek. This algorithm effectively combines the firefly algorithm and particle swarm optimization [46]. Inspired by the social behavior of fireflies, the firefly algorithm, along with the particle swarm optimization modeled after the movement and behavior of a flock, are robust techniques that have shown effectiveness in maneuvering complex optimization landscapes.

Our first objective is to delve into the core principles and mechanisms of these individual algorithms. This exploration will offer a comprehensive understanding of their operational dynamics, inherent strengths, and potential limitations. Once these foundational elements are understood, we then transition to a discussion on the integration of these two potent techniques into a unified hybrid model.

This convergence could potentially create a synergy, marrying the beneficial aspects of both methods. This union could possibly pave the way for exploring more efficient and effective solutions to intricate design problems. As we journey from understanding the fundamentals to conceptualizing a hybrid model, we aim to shed light on how optimization techniques can be innovatively adapted to meet specific challenges in design and planning. We hope to share these insights in this section.

I. OPTIMIZATION OF HRES WITH HOMER PRO SOFTWARE

HOMER Pro, often referred to as a hybrid optimization program, is a robust tool extensively employed for the sizing and optimization of diverse energy sources. The software is pivotal in executing a preliminary feasibility examination of a range of renewable energy configurations in various scales, and conducting sensitivity analyses for a spectrum of desired energy system configurations. Originated by the U.S. National Renewable Energy Laboratory (NREL), it caters to both on-grid and off-grid applications. The software operates on a Windows platform and is developed using C++ [47].The process of designing and structuring a microgrid presents a formidable challenge involving essential decision-making, including component sizing, design specifics, and the identification of an optimal location. Critical economic and technical data, such as inflation and interest rates and the technical characteristics of chosen components, form the cornerstone of these hybrid energy systems' cost appraisal.

Decision-making in this realm can be a complex task due to the array of technological possibilities and the varying accessibility of energy sources. HOMER Pro incorporates optimization and sensitivity algorithms to aid this evaluation process. The optimal solution generated by HOMER Pro is compliant with all user-defined limitations and achieves the minimum NPC. Moreover, HOMER Pro conducts an energy balance evaluation of the system, eliminating unviable system designs and demonstrating configurations that could potentially be utilized.

The simulation executed by HOMER Pro scrutinizes the technical feasibility of a system presumed to fulfill both electrical and thermal load needs, beyond various user-imposed

$$LPSP(\%) = \frac{\sum_{t=1}^{8760} P_{load}(t) - P_{PV}(t) - P_{WT}(t) + P_{DG}(t) + E_{BSmin}(t)}{\sum_{t=1}^{8760} P_{load}(t)} \tag{18}$$

constraints. Simultaneously, it examines the system's NPC, inclusive of installation and maintenance expenses. HOMER Pro conducts an exhaustive simulation of the hybrid energy system over 8760 hours (equivalent to a year) and proffers results in a tabular form. Each result set encompasses a selection of graphs and tables that elucidate their technical and economic virtues, thereby facilitating the comprehension and analysis of their techno-economic behavior and enabling a comparative study of different hybrid energy system configurations. These results can further be exported for more in-depth analyses.

The optimization procedure involves decision variables such as photovoltaic (PV) size, the quantity of wind turbines and batteries, converter size, presence of renewable energy sources encompassing PV and wind turbines, generator size, and a dispatch strategy dictating the system's operational methodology.

In the combined setting of HOMER Pro and MATLAB 2022b, the climatic and load data for a period of 8760 hours were employed, while ensuring the technical and economic parameters of the components remained at constant values. Concurrently, the decision variables specified in our objective function were optimized, adhering to the same values accepted within the MATLAB software. Figure 8 illustrates a single-line diagram representing the Hybrid Renewable Energy System (HRES). Furthermore, a detailed flowchart of the HOMER Pro simulation process is provided in Figure 9, offering an in-depth explanation of each step in the simulation.

J. PARTICLE SWARM OPTIMIZATION (PSO) ALGORITHM

Eberhardt and Kennedy proposed the stochastic and population based PSO algorithm depending on the global optimization technique in 1995, inspired by nature and developed according to the directions of the behaviors of swarms of birds [48]. PSO allowed the combination of the experiences of individuals and the experiences learned while working as a group, having obtained a simple model to solve challenging problems easily. The original PSO technique starts with a randomly initiated population, where the positions are updated via a velocity vector that contains the local and global best positions. The local best solution is the solution referring to the best fit value experienced by the particle. The global best solution the best fit value discovered by the aggregation of the particles in the swarm. Figure 10 presents the PSO algorithm's pseudo-code.

$$v_i^{t+1} = wv_i^t + c_1 \times r_1 \times \left(pbest_i(t) - x_i^t\right) + c_2 \times r_2 \times \left(gbest(t) - x_i^t\right) \quad (25)$$

$$x_i^{t+1} = x_i^t + v_i^{t+1} \quad (26)$$

For every time step, the goal of PSO is to accelerate each particle towards its optimal position using an arbitrarily weighted velocity factor. Each particle attempts to change its coordinates using equations and parameters. The present position, present velocities, proximity between the current position and pbest, proximity between the current position and gbest, the variance of velocity, and position of the particle can all be defined mathematically using Equations (25) and (26).

Here, $X_i(t)$ is instantaneous particle position, $X_i(t+1)$: next particle position, $V_i(t)$: instantaneous particle velocity, $V_i(t+1)$: velocity of the next particle, w: inertia weight value, $pbest_i(t)$: best "recalled" position, c_1 and c_2: scaling factors, and finally r_1 and r_2 are random numbers ranging from 0 to 1.

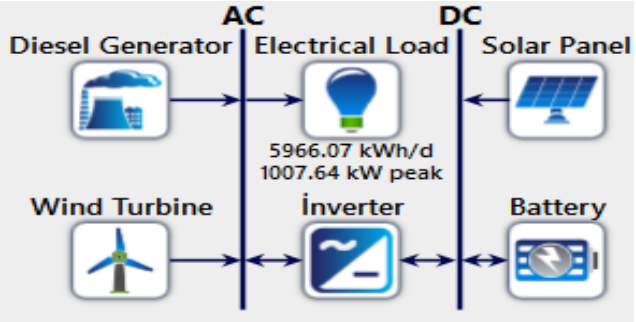

FIGURE 8. HOMERPro simulation model of solar PV, wind turbine, diesel generator, and battery hybrid energy system.

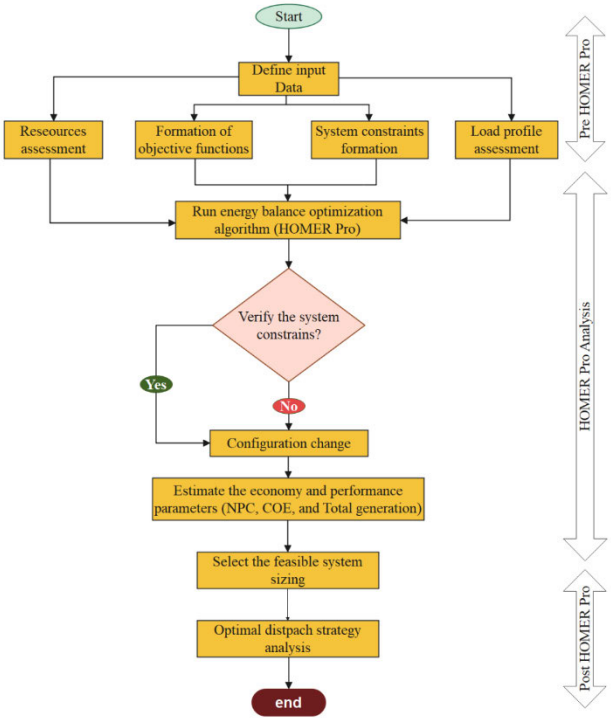

FIGURE 9. The HOMER Pro optimization flow diagram.

K. FIREFLY ALGORITHM (FA)

This algorithm is a metaheuristic optimization algorithm developed by Yang [49] in 2008, who is a mathematician. It was inspired by the fascinating light blinking behavior produced by some firefly species' bioluminescence. Although

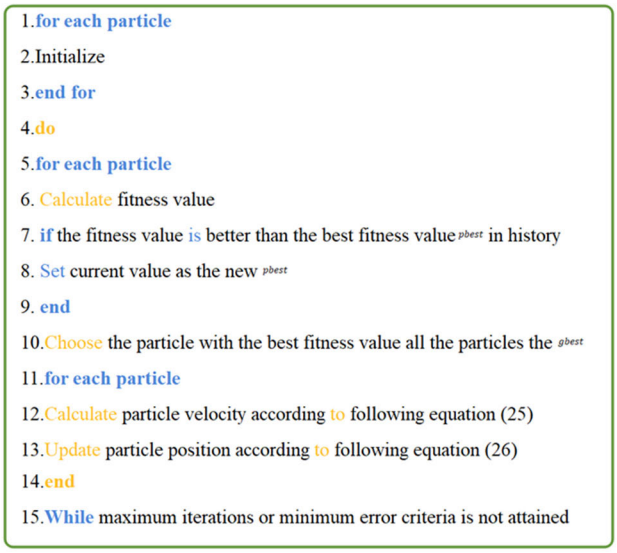

FIGURE 10. PSO algorithm pseudo-code.

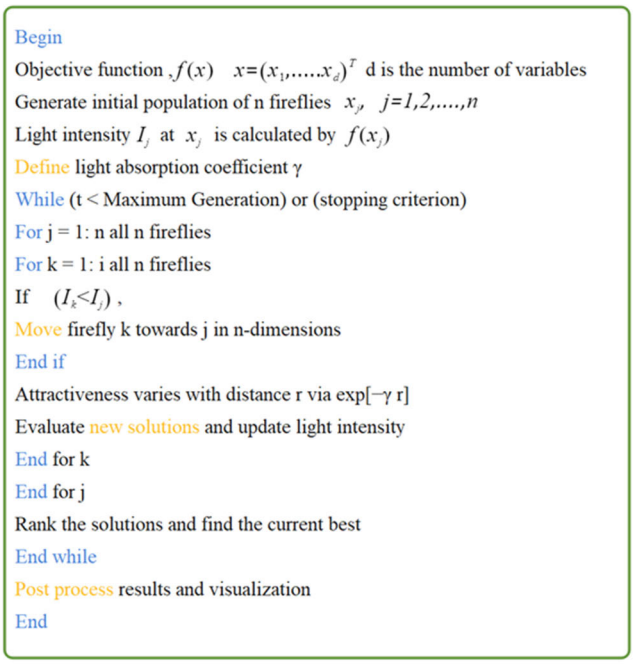

FIGURE 11. FA algorithm pseudo-code.

there are many similarities between this algorithm and other swarm intelligence-based algorithms, it is simpler in concept and implementation. The primary purpose of a firefly blinking its lights is to use it as a signaling system to attract other fireflies. Researchers suppose that flashing lights assist fireflies in finding possible mates, attracting preys, and guarding themselves from predatory animals. This algorithm was named after the fireflies that were used in its modeling. The point that fireflies are one sole specie and attract each other forms the basis of the algorithm.

In the FA, in order to obtain efficient optimum solutions, the objective function of a given optimization problem is related to the blinking light or light intensity that help the firefly swarm to navigate to brighter and more attractive places. All fireflies are considered a single genus. Therefore, male and female fireflies are no distinct, and all fireflies can attract each other. The brightness of fireflies is directly proportional to their desirability. As a result, the brighter a firefly is, the more appealing it is to other insects. As the distance between fireflies increases, so does the attraction. If one firefly in the environment is brighter than another, this firefly will move towards the brighter one [50]. They will move in random directions if there are no brighter fireflies nearby. Figure 11 summarizes the pseudocode of the FA.

The FA use two important criteria, these are light intensity and attractiveness. For simplicity, it is assumed that the brightness of a firefly determines its attractiveness. The variation of light intensity I_r by distance can be approximated using the Gaussian form below.

$$I_r = I_0 \times e^{-\gamma r^2} \tag{27}$$

I_r represents the light intensity, r represents the proximity of two fireflies, I_0 represents the initial light intensity, γ represents the coefficient light absorbance. Attractiveness of a firefly $\beta(r)$ could be determined since it is directly linked to the emitted light's intensity.

$$\beta_r = \beta_0 \times e^{-\gamma r^2} \tag{28}$$

where β_0 is the initial attractiveness defined at $r = 0$. The distance between any two fireflies i and j at x_i and x_j respectively is given by the Euclidean distance Equation (29).

$$r_{ij} = \left\| X_i - X_j \right\| = \sqrt{\sum_{k=1}^{d} \left(x_{i,k} - x_{j,k} \right)^2} \tag{29}$$

Here, $x_{i,k}$ represents i^{th} firefly's k^{th} component for its spatial coordinate x_i. When a firefly (i) is attracted to another (j), its movement is determined using

$$X_i^{t+1} = X_i^t + \beta_0 \times e^{-\gamma r^2} \left(X_j^t - X_i^t \right) + \alpha_t \times \varepsilon_t^t \tag{30}$$

where X_i^t is the current position of the i^{th} firefly, firefly's attractiveness is denoted by second term. The third term is randomization, which has a randomization parameter called α_t.

The following steps are involved in the implementation of the firefly algorithm for solving the constructed hybrid energy system design concept in this manuscript.

I. Reading (a) solar radiation, ambient temperature, wind speed data, and load demand (b) economic and technical details of the hybrid energy system components (c) parameters of the firefly algorithm and stopping criteria is the first step.
II. Create the firefly population at a random location in the n-dimensional search space (X_i). Define the coefficient of absorption, γ.
III. Using the defined objective function, compute each firefly's the light intensity, I_i.

IV. Make a comparison of each firefly's light intensity (X_i) with others (X_j).
V. In the case $I_i < I_j$, move X_i towards (X_j) by implementing Equation 30.
VI. Calculate the new objective function values for every firefly and adjust the intensity of light.
VII. Rank the fireflies to find the best one.
VIII. Repeat steps III through VII until you reach the criteria to stop.

L. HYBRID FIREFLY-PSO ALGORITHM (HFAPSO) ALGORITHM

A part of PSO is used in this section to improve FA convergence and also to improve the ability to not fall into local minima. Therefore, in the FAPSO method, local search is performed by a modified computation of mixed PSO properties as shown in Equations (31), (32) and (33). HFAPSO follows the same steps as FA, with the exception that FA's position vector is changed as follows: In HFAPSO, the distance between X_i and $pbest_i$ is the Cartesian distance.

$$r_{px} = \sqrt{\sum_{j=1}^{d} \left(pbest_{i,j} - X_{i,j}\right)^2} \tag{31}$$

$$r_{g,x} = \sqrt{\sum_{j=1}^{d} \left(gbest - X_{i,j}\right)^2} \tag{32}$$

$$X_i(t+1) = wX_i(t) + c_1 \times e^{-2_{px}} \left(pbest_i - X_i(t)\right) + c_2 \times e^{-2_{gx}} \left(gbest - X_i(t)\right) + \alpha \times \varepsilon_i \tag{33}$$

$$w = w_i - \left(\left(w_i - w_f\right)/iteration_{max}\right) \times iteration \tag{34}$$

$$f(i,t) = \begin{cases} true, \ if \ fitness \left(particle_i^t\right) \le gbest^{t-1} \\ false, \ if \ fitness \left(particle_i^t\right) > gbest^{t-1} \end{cases} \tag{35}$$

$$X_i(t+1) = X_i(t) + B_0 e^{-\gamma r_{ij}^2} \left(X_i(t) - gbest^{t-1}\right) + \alpha\varepsilon_i \tag{36}$$

$$V_i(t+1) = X_i(t+1) - X_{i\_temp} \tag{37}$$

A PSO operator transforms each particle's light intensity attraction step in the proposed method. In this step, each particle is drawn at random to the best position in the population. The modified attraction step of the HFAPSO algorithm performs local search in separate regions. The primary goal of the HFAPSO feature selection stage is to reduce the problem's features prior to supervised neural network categorization. Between all of the wrapper algorithms being used, HFAPSO, which solves optimization problems using methods based on the behavioral responses of fireflies, has emerged as an attractive algorithm.

It is already demonstrated that the PSO algorithm converges faster than others in certain problems. It is already demonstrated that the PSO algorithm converges faster than the others in some problems. Nevertheless, while it approaches the global optimal point, it tends to slow down. While the algorithm adapts itself to the global optimal position at every iteration, the danger of becoming trapped in the local optimum rises. The PSO algorithm's reliance on search criteria is yet another drawback. Diverse input parameters can result in varying convergence rates [51]. There are many versions of PSO algorithm introduced to improve performance. The key objective is to balance the aspects of exploration and exploitation. These include changes in evolution strategy, adjustment of parameters, changing update rules, as well as implementing stronger evolving strategies.

In the subsequent stage of the approach outlined in this paper, the velocity calculated utilizing Equation (25) will be replaced with the one calculated utilizing Equation (26) to update the particles' positions. In the case of this velocity being too low or too high, it could cause problems such as oscillation around the solution, causing the convergence rate to slow down. To resolve this, we must first set the inertia weight w and the acceleration coefficients (c_1, c_2),

Input: c_1, c_2 : Acceleration coefficients.
w:Inertia weight.
w_i, w_f: Initial and final values of linear decreasing inertia weight.
$random$: Random number generate function.
$fitness$: Fitness value calculate function.
$pbest, gbest$: Personal and global best positions.
X:Current positions of the particle.
X_{min}: Minimum search range limit.
X_{max}: Maximum search range limit.
V:Current velocities of the particle.
V_{min}: Minimum velocities limit.
V_{max}: Maximum velocities limit.
Pop:Size of the swarm.
D: Dimension of the particle.
t: Number of the current iteration.
$iteration_{max}$: Number of the maximum iteration.
Output : gbest particle and its fitness value.
Algorithm:
1. Initialize and assign input parameters $(c_1, c_2, w_i, w_f, X_{min}, X_{max}, V_{min}, V_{max}, D, Pop, iteration_{max})$
2. Randomly initialize position $X[Pop][D]$ matrix in the search range X_{min}, X_{max}
3. Randomly initialize velocity $V[Pop][D]$ matrix in the velocity range V_{min}, V_{max}
4. Calculate fitness $pbest$ and $gbest$ values
5. **While** Maximum Fitness Evaluations $(MaxFES = iteration_{max} \ x \ pop)$ limit is not reached do
6. **for** i:=1 to Pop **do**
7. **if** particle has an improvement in its fitness value in the last iteration according to Eq. (35) then
8. Save current particle position $(X_i(t))$ in a temp variable X_{i_temp}
9. Update particle position according to Eq.(36)
10. Update particle velocity according to Eq.(37)
11. **else**
12. Update intertia weight (w) according to Eq.(34)
13. Update particle velocity according to Eq.(25)
14. Update particle position according to Eq.(26)
15. **end if**
16. Check position and velocity range limitations
17. Calculate new particle fitness function value
18. **if** new particle fitness function value smaller than $pbest$ then
19. assign new $pbest$
20. **end if**
21. **if** new particle fitness function value smaller than $gbest$ then
22. assign new $gbest$
23. **end if**
24. **end for**
25. **end While**

FIGURE 12. HFAPSO algorithm pseudo-code.

TABLE 2. The optimization results obtained with the HOMERPro software tool for the hybrid energy system.

	Sceneraio1	Sceneraio2	Sceneraio3	Sceneraio4
Solar Panel(kW)	3067	3334	2540	2422
Wind Turbine(kW)	-	1	1	-
Diesel Generator (kW)	-	-	1200	1200
Battery (kW)	3601	3334	4489	4669
Converter (kW)	845	803	1128	1130
Net Present Cost (NPC)($)	9.69M	9.72M	10.4M	10.4M
Cost of Energy (COE)($)	0.274	0.275	0.293	0.294
Operating Cost ($ / *Year*)	335485	336703	349972	350795
Initial Cost($)	4.24M	4.25M	4.68M	4.70M

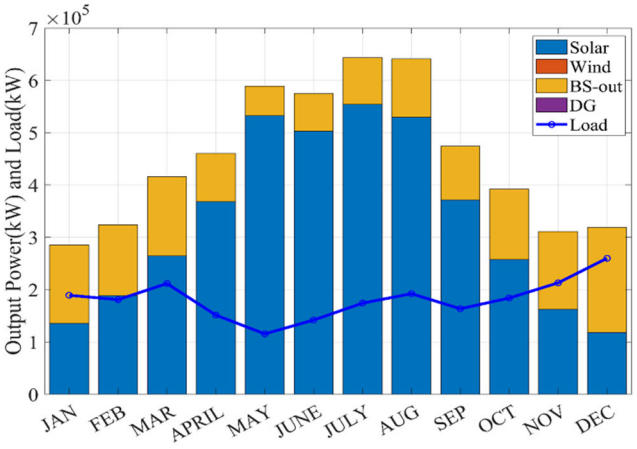

FIGURE 13. The monthly average power generated by the components of the PV/WT/DG/BS HRES in comparison with consumption.

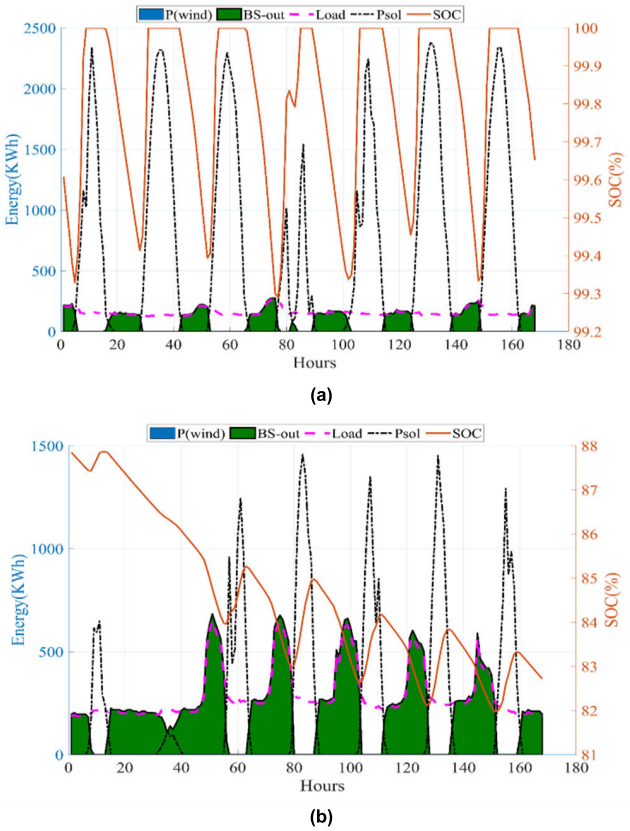

FIGURE 14. HRES Energy balance analysis (a) 3rd week of May, (b) 2nd week of January.

and later measure the velocity using Equation (25). These modifications are difficult: Although FA does not incorporate velocity in its algorithm, it has been demonstrated to be quite more efficient and successful in multimodal problems when compared to PSO [52]. The hybrid firefly and particle swarm optimization algorithm (HFAPSO) outlined by Aydilek is intended to capitalize on the strong points of both algorithms. The FA will handle local searches, whereas the PSO algorithm will aid in discovery. In the meantime, the inertia weight will be updated dynamically. The HFAPSO algorithm begins by initializing all of the parameters. The initialization of the particle positions and velocities will then be carried out at values that are random, in predetermined intervals. Fitness, global best (gbest), and personal best (pbest) will be calculated after that. The particle's fitness at this stage will then be evaluated by comparing it to the last iteration using Equation (35). If the particle's fitness value is not altered or increased, the FA assumes charge and a local search is launched; or else, the PSO algorithm follows Equations (25) and (26). When the FA algorithm is initiated, the position and velocity are determined using the Equations (36) and (37) respectively. The current position gets designated to a temporary variable described as (X_{i_temp}). The ranges of position and velocity of all fireflies and particles are then investigated in the subsequent stage. The position and velocity ranges of all fireflies and particles are then examined in the subsequent phase. The algorithm then gets stopped and the outcome becomes the output if the target value is met by the fitness value. Figure 12 presents the pseudocode used for the hybrid firefly-particle swarm optimization (HFAPSO).

IV. THE RESEARCH FINDINGS AND DISCUSSION

The optimization results obtained for a hybrid energy system composed of PV, wind, diesel, and battery components to meet the electrical load demand of the university central campus independently of the grid are evaluated using the methodology shown in Chapter 2. The research is carried out in four different scenarios. Despite the HOMERPro software results, the system is designed in the MATLAB environment using metaheuristic algorithms. The components are created differently in the scenarios proposed during the design stage. The 1st, 2nd, 3rd, and 4th scenarios are as follows:

TABLE 3. Sizing and cost results of optimum HRES obtained with PSO, GA, FA, and HFAPSO algorithms in different scenarios.

Scenarios	Optimization techniques	ACS ($)	NPC ($)	LCOE ($/kWh)	Total Gases Emissions (kg/year)	Renewable Fraction (%)	Wind turbine (kW)	Solar Power (kW)	Total DG Energy Generation (kWh)	Battery Units
Scenario1	PSO	480302.96	7793299.10	0.2205	-	100	-	2460.4289		3579.2674
	GA	484625.02	7863495.81	0.2225	-	100	-	3226.8322		2674.2066
	FA	481617.90	7814655.59	0.2211	-	100	-	3072.0781		2827.0878
	HFAPSO	479340.57	7777668.32	0.2201	-	100	-	2787.3411		3153.9405
Scenario 2	PSO	484857.71	7867275.10	0.2226	-	100	1	3300.0424	-	2579.5634
	GA	485029.90	7870071.71	0.2227	-	100	1	3226.8322	-	2674.2066
	FA	482123.53	7822867.88	0.2213	-	100	1	3081.7097	-	2816.3635
	HFAPSO	480226.03	7792049.58	0.2205	-	100	1	2807.3194	-	3127.4924
Scenario 3	PSO	521514.52	8462637.15	0.2394	691240.2	99.95	-	2965	990.7129	2935
	GA	521892.41	8468774.61	0.2396	670347.6	99.95		3005	960.7687	2890
	FA	513575.46	8333694.71	0.2358	450957.3	99.97	-	3000	646.3299	2900
	HFAPSO	513410.63	8331017.58	0.2357	587987.4	99.96	-	2997.6213	842.7268	2900
Scenario 4	PSO	616633.78	10007517.76	0.2831	2057958.2	99.85	21.7634	3400	2949.5473	2450
	GA	616644.59	10007693.25	0.2831	2057986.8	99.85	21.7599	3400	2949.5884	2450
	FA	625965.38	10159077.03	0.2874	2057493.5	99.86	45.8636	3395.2677	2948.8813	2450
	HFAPSO	604794.71	9815233.36	0.2777	1464149.3	99.89	93.2842	3400	2098.4769	2450

TABLE 4. Energy and cost results of optimum HRES obtained with PSO, GA, FA, HFAPSO algorithms in different scenarios1 and scenarios2.

Description	Scenario 1(PV+Bat)				Scenario 2(PV+WT+Bat)			
	PSO	GA	FA	HFAPSO	PSO	GA	FA	HFAPSO
Total Wind Energy (kWh)	-	-	-	-	125.57	125.57	125.57	125.57
Total Solar Energy (kWh)	3564111.2	4674302.5	4450129.9	4037667.6	4780352.8	4674302.5	4464082.0	4066607.64
Wasted Energy (kWh)	1412303.8	2452923.8	2241504.9	1853758.5	2553061.4	2453047.2	2254778.4	1880852.8
Total Load Demand(kWh)	2177615.49	2177615.49	2177615.49	2177615.49	2177615.49	2177615.49	2177615.49	2177615.49
BS input Energy (kWh)	1321116.61	1350261.96	1344364.96	1333852.5	1353131.8	1350204.5	1344668.5	1334677.5
BS output Energy (kWh)	1461325.1	1420899.1	1427755.9	1441959.3	1417724.3	1420833.0	1427248.8	1440811.9
WT REF (%)	-	-	-	-	0.003	0.003	0.003	0.004
PV REF (%)	100	100	100	100	99.997	99.997	99.997	99.996
Wind Cost($)	-	-	-	-	6575.90	6575.90	6575.90	6575.90
Solar Cost($)	3597333.1	4717872.7	4491610.4	4075303.5	4824911.5	4717872.7	4505692.6	4104513.3
Diesel Generator Cost($)	-	-	-	-	-	-	-	-
Battery Cost ($)	4153818.3	3103475.4	3280897.4	3660217.1	2993639.99	3103475.42	3268451.65	3629523.53
Inverter Tcost ($)	42147.6	42147.6	42147.6	42147.6	42147.6	42147.6	42147.6	42147.6

TABLE 5. Energy and cost results of optimum HRES obtained with PSO, GA, FA, HFAPSO algorithms in different scenarios3 and scenarios4.

Description	Scenario 3(PV+DG+Bat)				Scenario 4 (PV+WT+DG+Bat)			
	PSO	GA	FA	HFAPSO	PSO	GA	FA	HFAPSO
Total Wind Energy(kWh)	-	-	-	-	2732.9	2732.4	5759.3	11714.1
Total Solar Energy(kWh)	4295019.4	4352962.3	4345719.5	4342273.8	4925148.7	4925148.7	4918293.7	4925148.7
Wasted Energy(kWh)	2095609.8	2150112.8	2143300.2	12140059.2	2694022.7	2694022.3	2690486.8	2702990.8
Total Load Demand(kWh)	2177615.49	2177615.49	2177615.49	2177615.49	2177615.49	2177615.49	2177615.49	2177615.49
BS input Energy (kWh)	1340227.4	1341737.4	1341545.7	341454.8	1354266.1	1354266.2	1352753.57	1350136.4
BS output Energy (kWh)	1431843.1	1429943.1	1430496.2	1430413.5	1409332.7	1409332.9	1407957.7	1405578.5
WTREF (%)	-	-	-	-	0.05	0.05	0.12	0.23
PV REF (%)	99.95	99.95	99.97	99.96	99.80	99.80	99.74	99.66
Wind Cost ($)	-	-	-	-	143114.0	143091.3	301594.9	613428.2
Solar Cost ($)	4335054.1	4393537.2	4386226.8	4382749.1	4971057.1	4971057.1	4964138.1	4971057.0
Diesel Generator Cost($)	679303.4	679181.3	539806.6	540607.2	2007920.2	2008118.4	2007917.5	1345321.6
Battery Cost ($)	3406131.8	3353908.3	3365513.6	3365513.6	2843278.7	2843278.7	2843278.7	2843278.7
Inverter Tcost ($)	42147.6	42147.6	42147.6	42147.6	42147.6	42147.6	42147.6	42147.6

•Scenario 1: It is carried out with solar panels and battery banks. (PV+BS)

•Scenario 2: It is carried out with wind turbines, solar panels, and battery components. (PV+WT+BS)

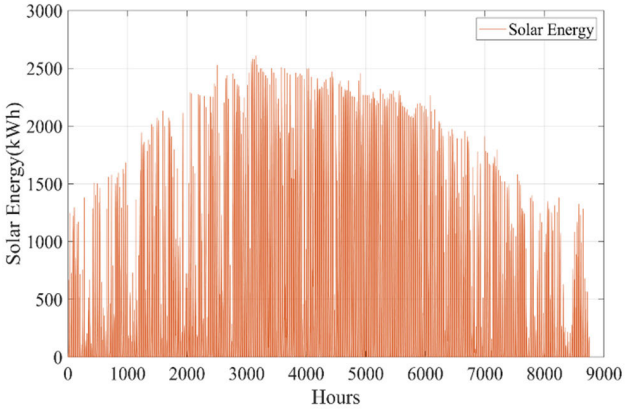

(a)

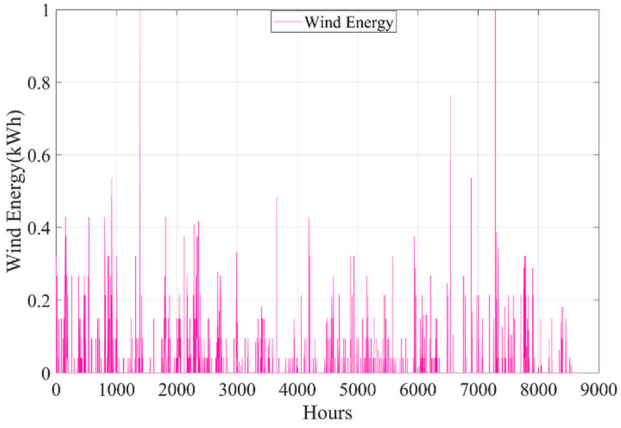

(b)

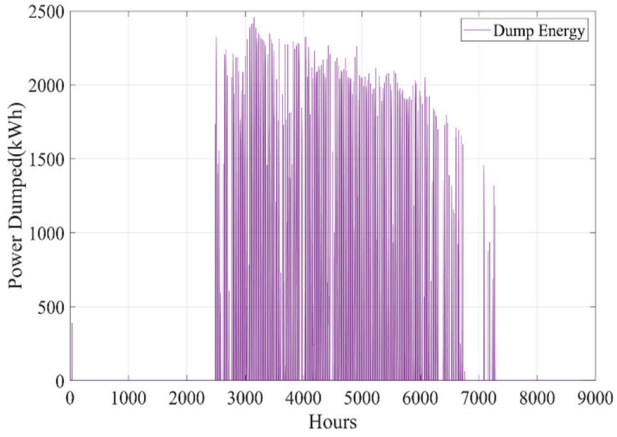

(c)

FIGURE 15. (a) PV array's power output. (b) WT's power output (c) Renewable energy sources' energy surplus.

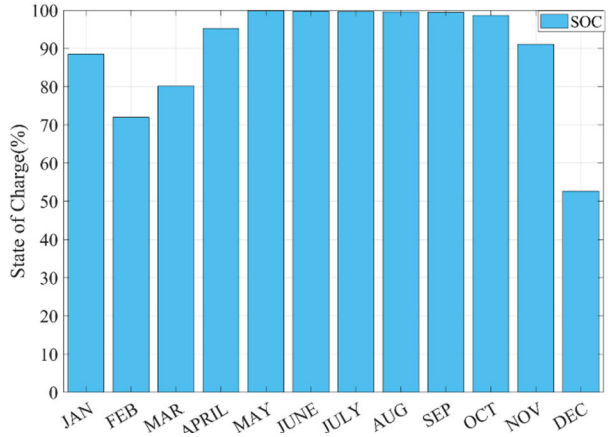

(a)

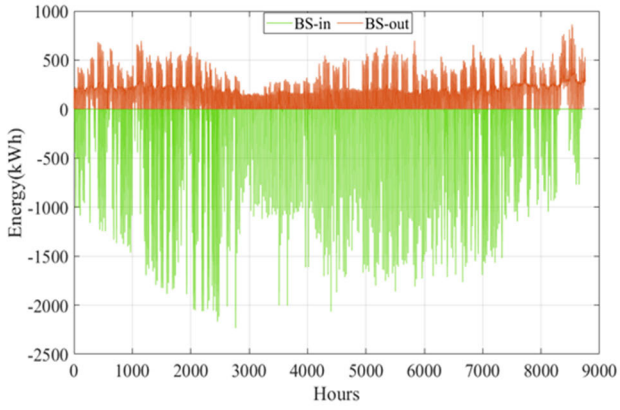

(b)

FIGURE 16. (a) The monthly average SOC (%) of the optimized system (b) Annual battery energy balance(kWh).

•Scenario 3: It is carried out with solar panels, diesel generators, and battery banks. (PV+DG+BS)

•Scenario 4: It is carried out with solar panels, wind turbines, diesel generators, and batteries (PV+WT+ DG+BS)

Table 2 shows that the optimal configuration achieved through HOMERPro software optimization involves 3067 kW solar panels, 3601 kW batteries, and 845 kW inverters. This configuration results in a NPC of 9.69 million dollars and a unit energy cost of 0.274 ($). Tables 3, 4, and 5 show the optimal results obtained by the proposed HFAPSO in comparison to the previously mentioned PSO, GA, and FA algorithms. After the comparison of these four different scenarios, it is clear that scenario 1's 2787.3411 kW PV and 3153.9405 kW battery provide the best configuration to meet the load demand of the proposed HFAPSO. The ACS for this configuration is $479340.57, the NPC is $7777668.22, and the LCOE is $0.2201 kWh. PSO comes in second with an LCOE of $0.2205 kWh, and FA comes in third with $0.2211 kWh. The worst approach, on the other hand, is GA, because a 3226.8322 kW PV panel with a $0.2225 kWh LCOE requires a 2,674.2066-kW battery. These findings support the proposed HFAPSO's superiority in determining the optimal size of the hybrid RES integrated microgrid. Figure 13 depicts annual demand as power generated by each component of the approaches used. When PV panels produced less power in January, November, and December, batteries were introduced to meet the power demand. More solar energy was produced in the remaining months as natural resources became more abundant. Because energy resources

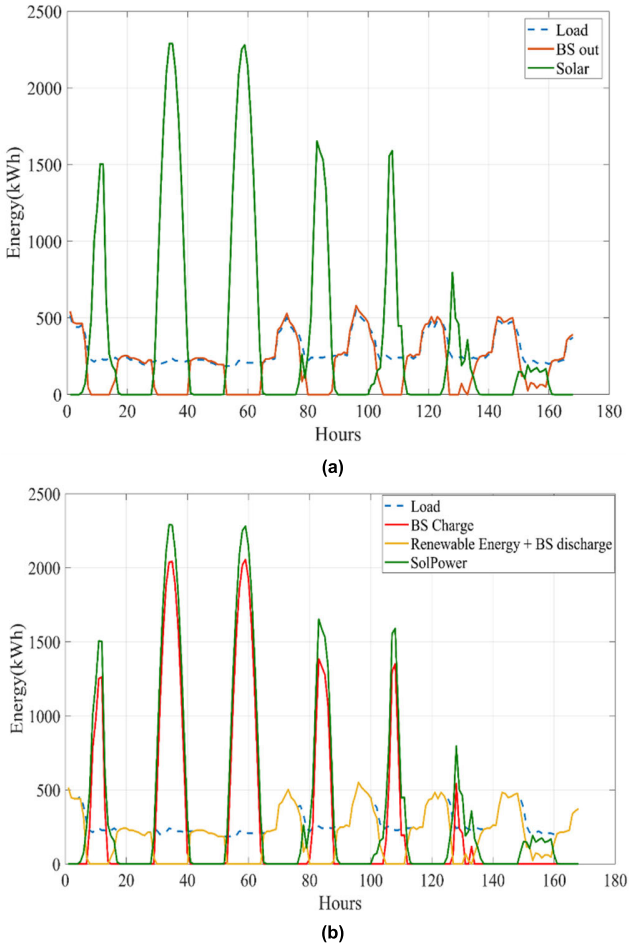

FIGURE 17. Comparison of HRES's optimum Scenario 1 load demand and energy resources.

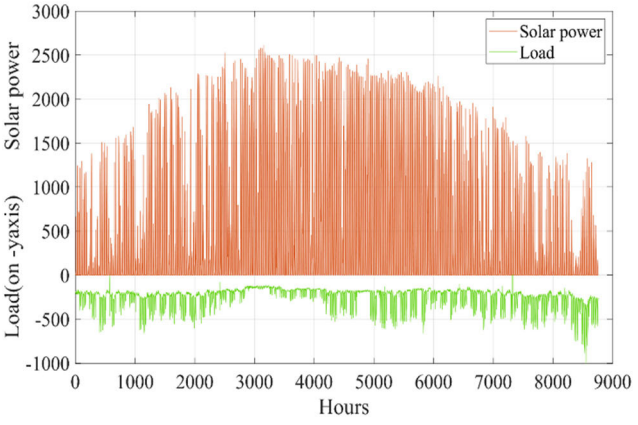

FIGURE 18. Annual profile of solar energy generation and load demand.

became more plentiful during the rest of the period, more solar energy was generated. In addition, because less power is drawn in the summer, there have been a decrease in the use of battery banks. Provided graph also shows an excess of energy. It is clear that all approaches were able to withstand the strain. The proposed HFAPSO, on the other hand, reveals

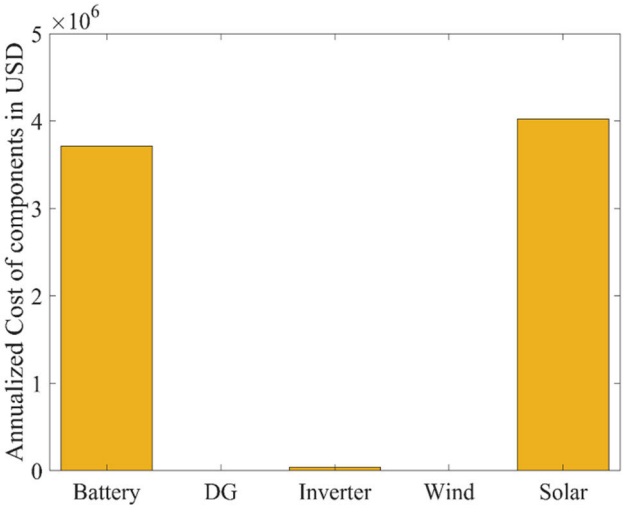

FIGURE 19. Costs results of HRES design using scenario 1.

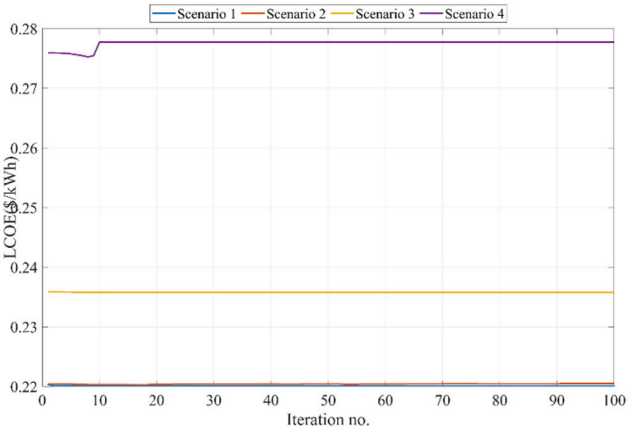

FIGURE 20. LCOE convergence for scenarios (1-4).

the preferred economic nature of the microgrid because it does not have a large excess of power like other approaches. This validates the dependable microgrid to ensure safe and cost-effective operation. Figure 14 (a)–(b) depicts the weekly balance of power obtained via HFAPSO when the load is lower in the 3rd week of May and higher in the 2nd week of January. Because the power generated by renewable energy sources is low in January, SOC of the battery approaches SOCmin, and it is at SOCmax in May because the power generation is high. As a result, it is concluded that the proposed approach falls within certain parameters that allow it to be properly dimensioned. This proposed approach should be investigated in various RES configurations. As a result, sensitivity analysis is presented, and the proposed approach is tested on microgrids with various architectures. Scenario 1 (PV+BS), Scenario 2 (PV+WT+BS), Scenario 3 (PV+DG+BS), and Scenario 4 (PV+WT+BS+DG) were investigated. Due to their performance, these systems are optimized using the proposed PSO, FA, and GA compared to other approaches reported outside of HFAPSO.

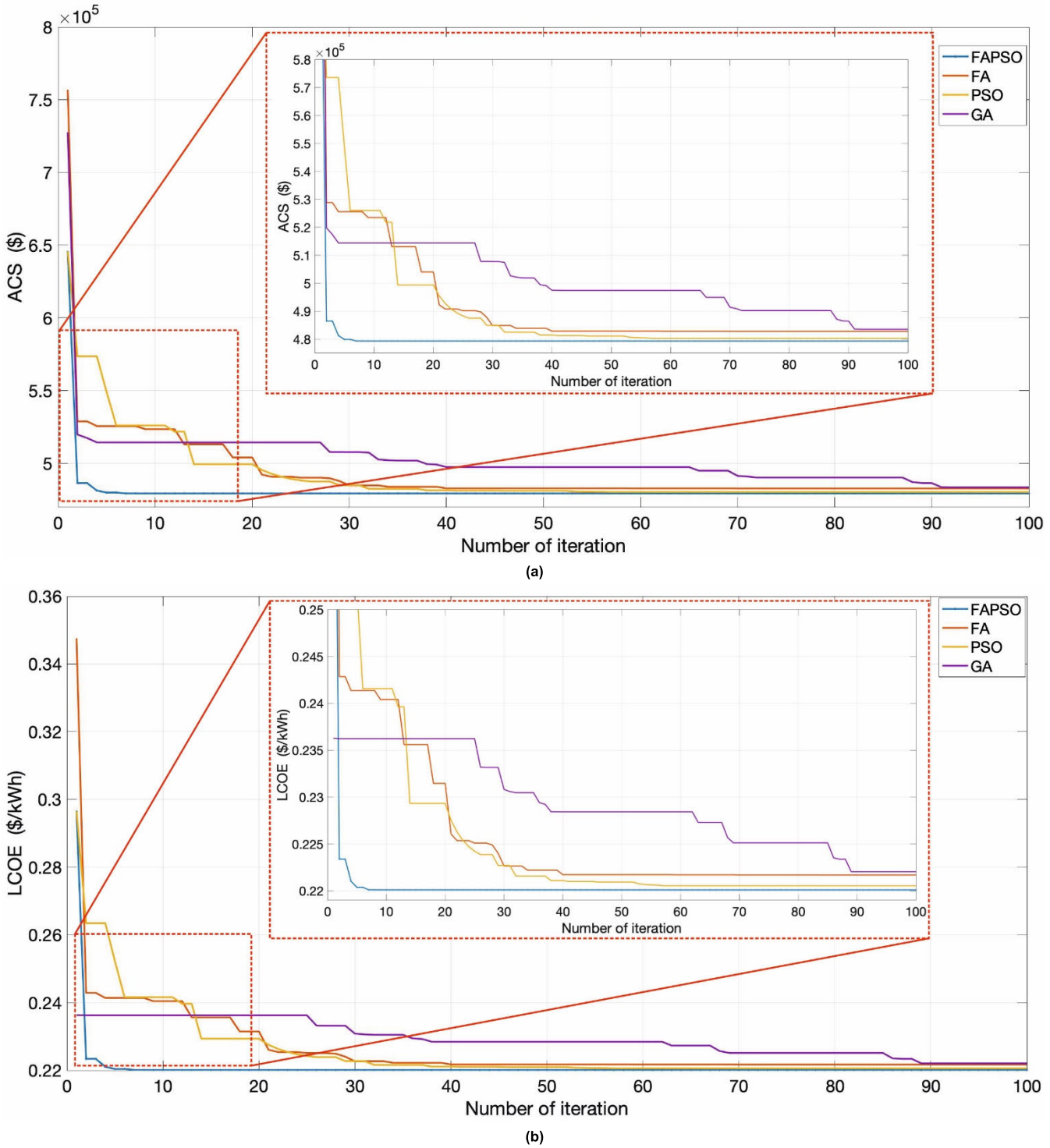

FIGURE 21. The convergence time of HFAPSO compared to the GA, FA, PSO metaheuristic techniques a) ACS b) LCOE c) NPC.

Scenarios 1 and 2 have the lowest TGE emissions, however, due to the use of 100% renewable energy sources, hybrid systems in scenarios 3 and 4 produce the highest amount of gas emissions. Güven and Samy proposed a hybrid energy system based on solar/wind/biomass/fuel cell sources in their study, and the optimization results showed a TGE value of approximately 521 tons/year. However, in scenario 1 and scenario 2 presented in this study, the TGE value is zero. The TGE value is commonly used to measure the environmental impact of an energy system or process, and a lower TGE value

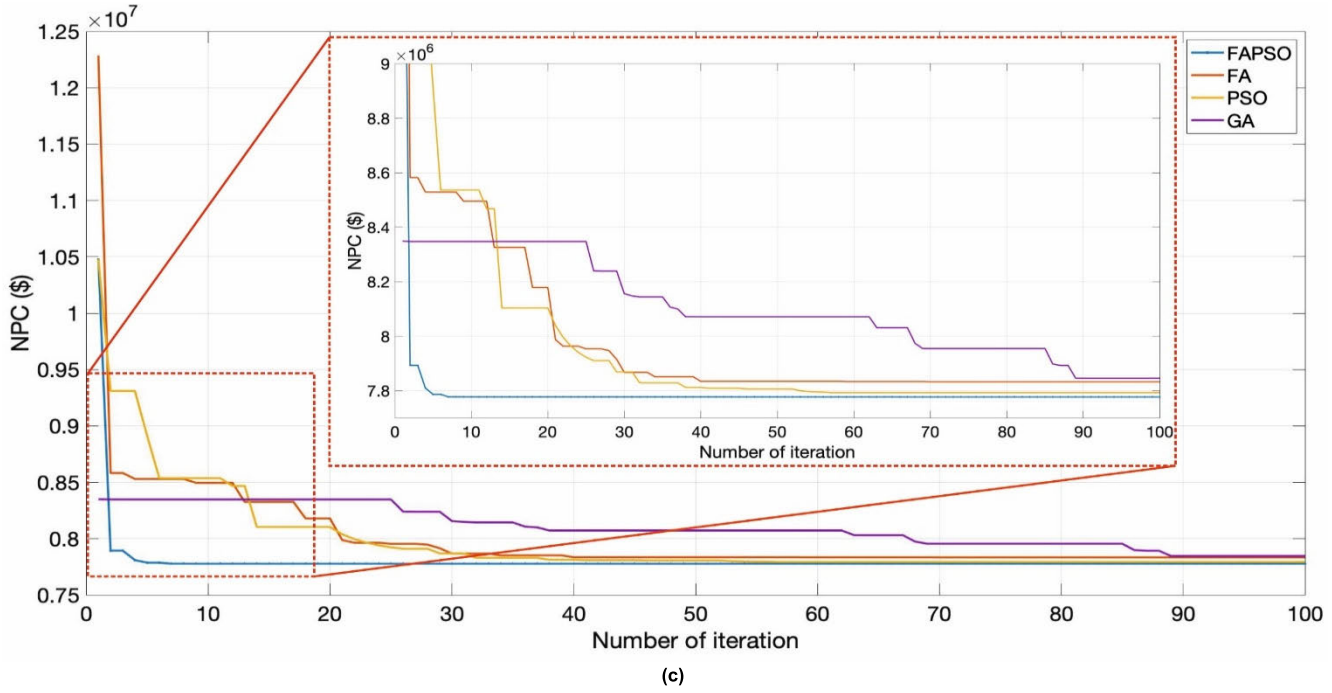

FIGURE 21. *(Continued.)* **The convergence time of HFAPSO compared to the GA, FA, PSO metaheuristic techniques a) ACS b) LCOE c) NPC.**

indicates better environmental sustainability of the sources used in the study [40].

Tables 4 and 5 show the output power values for solar panels and wind turbines, as well as the excess energy generated by these sources, for all scenarios. Figure 15 (a), (b), and (c) show the HRES's energy profile over the course of the year. After the load demand is met, solar energy sources produce 1853758.5 kWh of waste energy. This extra energy will be used for deferred loads such as irrigation pumping systems on campus.

SOC is an important parameter to consider because the battery is used as a storage source in the hybrid energy system. Figure 16 (a) depicts the battery's average SOC. According to this, occupancy rates in January were 88.48%, 71.98% in February, 80.06% in March, 95.17% in April, 91.04% in November, 52.624% in December, and 100% in the remaining months. Figure 16 (b) furthermore demonstrates that the battery SOC is usually good, with some exceptions, including when natural resources are scarce in January-December also when load demand is higher in June, July, and August. Furthermore, the battery's charge - discharge rates must be constantly monitored.

Figure 17 (a) and (b) depict a weekly graph of how the hybrid energy system's load demand is met. First and foremost, because the best result is scenario 1 (PV+Bat), solar energy and batteries meet the entire load requirement in this operational strategy. The batteries would discharge if the solar radiation's production of renewable energy did not meet the load demand and the batteries were full enough to meet the additional load demands. When the battery and renewable energy sources fail to meet load requirements, the diesel generator launches in to fill the energy gap. The exception of Figure 17 (b) graph is that it presents an additional battery charging line to Figure 17 (a). Figure 17 (b) shows that if there is enough solar power, the battery will charge. This, in turn, is charged with any excess energy generated by the solar energy source at the time.

Figure 18 compares solar power generation and load requirements as a result of the HRES scenario1. The load demand is met here, and there is also an excess of energy production. Figure 19 also depicts the costs of the system components. A solar panel costs 4075303.5 dollars, a battery costs 3660217.1 dollars, and an inverter costs 2147.6 dollars in this country. The LCOE convergence curves for the various study scenarios are depicted in Figure 20. All scenarios, with the exception of scenarios 3 and 4, have convergence curves that perform well in this study.

If an algorithm's fitness curve shows a faster decrease than other algorithms, it means that this algorithm performs better. Similarly, when fitness curves are examined, it can be seen how stable the algorithms are during the optimization problem solution and how accurate the solution is. Therefore, comparing the fitness curves of algorithms can be used as an important indicator to determine which algorithm performs better. However, in addition to fitness curves, factors such as the speed of algorithms, memory usage, and other factors should also be considered. Figure 21 depicts convergence curves that show how HRES approaches the most optimal solution as a result of optimization with the HFAPSO algorithm. The structure/slope of this curve indicates that

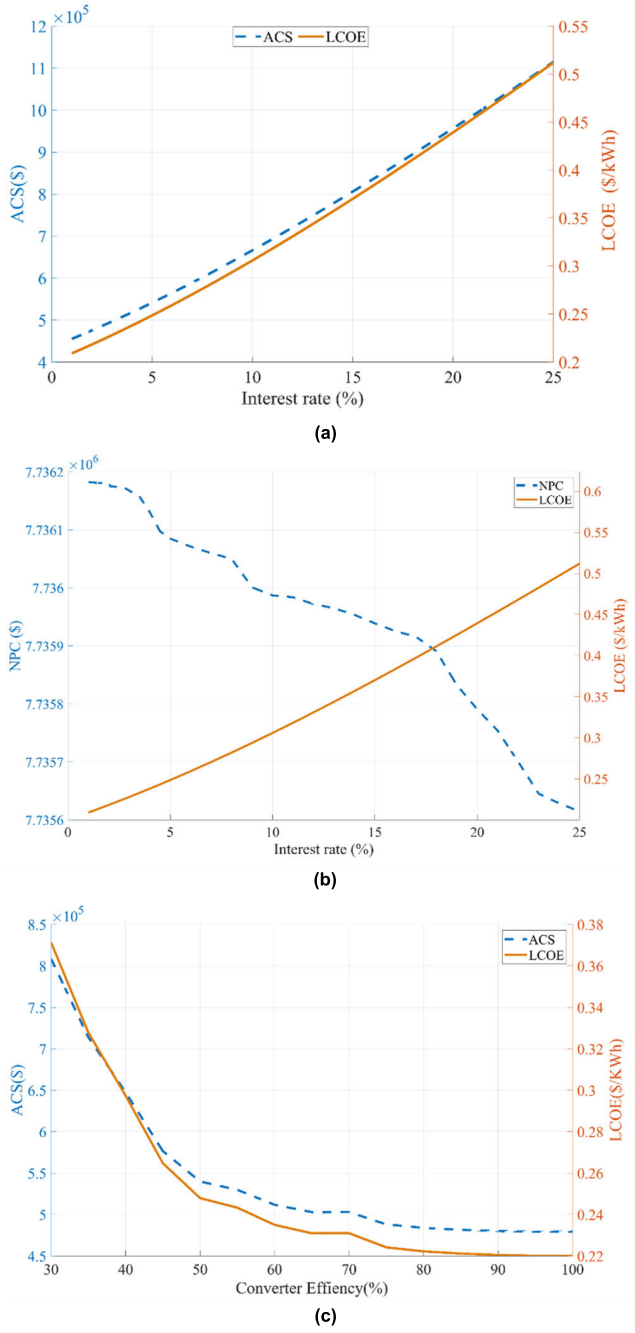

FIGURE 22. Effect of varying the interest rate on ACS and LCOE b) Effect of varying the interest rate on NPC and LCOE c) Effect of converter efficiency on LCOE value.

the algorithms converge to the optimal solution very quickly against iterations. Figure 21 (a) (b) (c) depicts the optimization algorithms' performance for annual ACS, LCOE, and NPC convergence values, respectively. When compared to the other four algorithms, the hybrid HFAPSO algorithm used here converges quickly after the fifth iteration. As a result, it is clear that this algorithm completes the calculations in HRES optimizations quickly, providing the best results.

Sensitivity analysis in hybrid energy systems is a type of analysis performed to determine the impact of changing the key parameters that determine the system's performance. This analysis is used to understand how system performance may vary under different scenarios. For example, it can be used to examine how the system may be affected by different weather conditions, load demands, or component failures. This allows for more accurate and reliable decision-making in the design and operation of the system. To explore the impact of modifying the interest rate on the cost of the proposed microgrid, interest rate values (1%, 5%, 10%, 13%, and 15%) are ranged from the base value (2.07%) for which the system was designed, and the optimization process is repeated.

Figures 22 (a) depict the change in the system's ACS and LCOE values during the interest rate change. From here, it can be seen that the increase is proportional to the ACS and LCOE interest rates. Figure 22 (b) represents the level and rate of change in the total NPC of the proposed microgrid as a result of interest rate changes, uncovering an inverse correlation between NPC interest rates.

The amount and rate of change in the LCOE and ACS values of the proposed microgrid as a result of converter efficiency changes are shown in Figure 22 (c), which illustrates an inverse relationship between converter efficiency-based ACS and LCOE. The value of ACS and LCOE falls as the inverter's efficiency rises. According to the study sensitivity displayed in Figure 22, the discount rate and converter efficiency have a substantial impact on the value of NPC,LCOE and ACS.

V. CONCLUSION

This study proposed a conceptual mathematical model to optimize the size and composition of off-grid hybrid energy components - PV, WT, BS, and DG using a hybrid HFAPSO algorithm that combines FA and PSO. The primary objective of the optimization problem was to meet the total energy requirement of an off-grid university campus, minimize the total annual system cost, and determine the optimal number of PV-panels, wind turbine panels, and batteries required. The advantageous aspects of PSO and FA were blended in an attempt to mitigate the shortcomings of these algorithms, such as early convergence and local optima. The hybrid use of these algorithms achieved a balance between the processes of discovery and exploitation.

The output from the HFAPSO algorithm was compared with results from HOMERPro, GA, FA, and PSO, demonstrating that the proposed algorithm provides superior outcomes. While HOMERPro simulates the proposed system in hours, these algorithms reduced this duration to minutes. The optimal hybrid system, without violating any constraints, satisfactorily meets the load demand using only solar power, wind, and batteries, with the majority of the contribution coming from solar power. Instantaneous energy analysis results were made readily available with the help of energy graphics that supported the technical results in the study.

In addition, the geopolitical implications on the cost of fossil fuels, particularly in Europe, were also considered. The proposed HFAPSO algorithm significantly reduced the dependency on fossil fuels, thus minimizing their economic impact. This approach aligns with the imperative for emission reductions in the current global scenario. The study emphasized the importance of renewable energy systems and the role they play in environmental sustainability, cost-effectiveness, and energy reliability.

The HFAPSO algorithm proved more advantageous than the FA and PSO optimization algorithms in terms of both computational cost and complexity. The fast solution generation capability and the ability to approach the global optimum of the HFAPSO algorithm in this problem were confirmed. The adaptive feature of this algorithm also allowed for solutions suitable for the problem size.

Conclusively, the use of the HFAPSO algorithm provided significant benefits in designing HRESs, with resulting ACS: 479340.57 $, LCOE: 0.2201 $, NPC: 7777668.32 $, REF: 100%. The proposed algorithm significantly contributes to solving the design problems of HRESs and offers substantial advantages. The results of this comprehensive study indicate that the presented algorithm effectively and efficiently addresses the optimal design issues for hybrid renewable energy systems, contributing significantly to avoiding unnecessary investments and the effective use of resources.

This study makes a significant contribution to the optimization of off-grid hybrid renewable energy systems. However, there are potential paths for future research to go even further. Firstly, it would be beneficial to model in more detail how energy demand changes over time. This could help us better understand how increases in energy demand at specific times impact the optimization of hybrid renewable energy systems. Additionally, it would be useful for future studies to test the proposed HFAPSO algorithm in different geographical locations, places with different weather conditions, or situations with varying energy demands. Lastly, examining in more detail how uncertainty factors affect this algorithm could further enhance the robustness and general applicability of the study.

REFERENCES

[1] M. Mehrpooya and M. M. M. Sharifzadeh, "A novel integration of oxy-fuel cycle, high temperature solar cycle and LNG cold recovery—Energy and exergy analysis," *Appl. Thermal Eng.*, vol. 114, pp. 1090–1104, Mar. 2017, doi: 10.1016/j.applthermaleng.2016.11.163.

[2] D. S. Koussa and M. Koussa, "GHGs (greenhouse gases) emission and economic analysis of a GCRES (grid-connected renewable energy system) in the arid region, Algeria," *Energy*, vol. 102, pp. 216–230, May 2016, doi: 10.1016/j.energy.2016.02.103.

[3] H. Yang, W. Zhou, L. Lu, and Z. Fang, "Optimal sizing method for stand-alone hybrid solar–wind system with LPSP technology by using genetic algorithm," *Sol. Energy*, vol. 82, no. 4, pp. 354–367, Apr. 2008, doi: 10.1016/j.solener.2007.08.005.

[4] O. Nadjemi, T. Nacer, A. Hamidat, and H. Salhi, "Optimal hybrid PV/wind energy system sizing: Application of cuckoo search algorithm for Algerian dairy farms," *Renew. Sustain. Energy Rev.*, vol. 70, pp. 1352–1365, Apr. 2017, doi: 10.1016/j.rser.2016.12.038.

[5] F. Akram, F. Asghar, M. A. Majeed, W. Amjad, M. O. Manzoor, and A. Munir, "Techno-economic optimization analysis of stand-alone renewable energy system for remote areas," *Sustain. Energy Technol. Assessments*, vol. 38, Apr. 2020, Art. no. 100673, doi: 10.1016/j.seta.2020.100673.

[6] A. M. Hemeida, A. S. Omer, A. M. Bahaa-Eldin, S. Alkhalaf, M. Ahmed, T. Senjyu, and G. El-Saady, "Multi-objective multi-verse optimization of renewable energy sources-based micro-grid system: Real case," *Ain Shams Eng. J.*, vol. 13, no. 1, Jan. 2022, Art. no. 101543, doi: 10.1016/j.asej.2021.06.028.

[7] S. Younsi, O. Kahouli, N. Hamrouni, H. Alsaif, A. Aloui, and S. Hamed, "Performance analysis and multi-mode control of grid connected micro wind–solar hybrid generator in Saudi Arabia," *J. Taibah Univ. Sci.*, vol. 16, no. 1, pp. 550–565, Dec. 2022, doi: 10.1080/16583655.2022.2078134.

[8] T. Chowdhury, H. Chowdhury, S. Hasan, M. S. Rahman, M. M. K. Bhuiya, and P. Chowdhury, "Design of a stand-alone energy hybrid system for a makeshift health care center: A case study," *J. Building Eng.*, vol. 40, Aug. 2021, Art. no. 102346, doi: 10.1016/j.jobe.2021.102346.

[9] D. T. Hermann, T. K. F. Armel, T. René, and N. Donatien, "Consideration of some optimization techniques to design a hybrid energy system for a building in Cameroon," *Energy Built Environ.*, vol. 3, no. 2, pp. 233–249, Apr. 2022, doi: 10.1016/j.enbenv.2021.01.007.

[10] S. Poonam, P. Manjaree, and S. Laxmi, "Comparison of traditional and swarm intelligence based techniques for optimization of hybrid renewable energy system," *Renew. Energy Focus*, vol. 35, pp. 1–9, Dec. 2020, doi: 10.1016/j.ref.2020.06.010.

[11] P. Das, B. K. Das, M. Rahman, and R. Hassan, "Evaluating the prospect of utilizing excess energy and creating employments from a hybrid energy system meeting electricity and freshwater demands using multi-objective evolutionary algorithms," *Energy*, vol. 238, Jan. 2022, Art. no. 121860, doi: 10.1016/j.energy.2021.121860.

[12] C. Mokhtara, B. Negrou, N. Settou, B. Settou, and M. M. Samy, "Design optimization of off-grid hybrid renewable energy systems considering the effects of building energy performance and climate change: Case study of Algeria," *Energy*, vol. 219, Mar. 2021, Art. no. 119605, doi: 10.1016/j.energy.2020.119605.

[13] M. S. Dehaj and H. Hajabdollahi, "Multi-objective optimization of hybrid solar/wind/diesel/battery system for different climates of Iran," *Environ., Develop. Sustainability*, vol. 23, no. 7, pp. 10910–10936, Jul. 2021, doi: 10.1007/s10668-020-01094-1.

[14] W. Zhu, J. Guo, and G. Zhao, "Multi-objective sizing optimization of hybrid renewable energy microgrid in a stand-alone marine context," *Electronics*, vol. 10, no. 2, pp. 1–24, 2021, doi: 10.3390/electronics10020174.

[15] M. S. Javed, A. Song, and T. Ma, "Techno-economic assessment of a stand-alone hybrid solar-wind-battery system for a remote island using genetic algorithm," *Energy*, vol. 176, pp. 704–717, Jun. 2019, doi: 10.1016/j.energy.2019.03.131.

[16] L. Chen, S. Wang, and N. Yousefi, "An optimal arrangement for photovoltaic/diesel/battery management system applying crow search algorithm: A case of Namib desert," *Int. J. Ambient Energy*, vol. 43, no. 1, pp. 4977–4989, Dec. 2022, doi: 10.1080/01430750.2021.1909130.

[17] R. Saraswat and S. Suhag, "Optimal economic sizing of stand-alone hybrid renewable energy system (HRES) suiting to the community in Kurukshetra, India," *Int. J. Comput. Digit. Syst.*, vol. 12, no. 1, pp. 801–812, Sep. 2022.

[18] B. K. Das, R. Hassan, M. S. H. K. Tushar, F. Zaman, M. Hasan, and P. Das, "Techno-economic and environmental assessment of a hybrid renewable energy system using multi-objective genetic algorithm: A case study for remote island in Bangladesh," *Energy Convers. Manage.*, vol. 230, Feb. 2021, Art. no. 113823, doi: 10.1016/j.enconman.2020.113823.

[19] Y. Liu, D. Zhang, and H. B. Gooi, "Optimization strategy based on deep reinforcement learning for home energy management," *CSEE J. Power Energy Syst.*, vol. 6, no. 3, pp. 572–582, Sep. 2020, doi: 10.17775/CSEEJPES.2019.02890.

[20] E. Foruzan, L.-K. Soh, and S. Asgarpoor, "Reinforcement learning approach for optimal distributed energy management in a microgrid," *IEEE Trans. Power Syst.*, vol. 33, no. 5, pp. 5749–5758, Sep. 2018, doi: 10.1109/TPWRS.2018.2823641.

[21] A. Morteza, S. Sadeghi and S. Taheri, "Deep learning hyperparameter optimization: Application to electricity and heat demand prediction for buildings," *Energy Buildings*, vol. 289, Jun. 2023, Art. no. 113036, doi: 10.2139/ssrn.4349044.

[22] H. J. Kim and M. K. Kim, "A novel deep learning-based forecasting model optimized by heuristic algorithm for energy management of microgrid," *Appl. Energy*, vol. 332, Feb. 2023, Art. no. 120525, doi: 10.1016/j.apenergy.2022.120525.

[23] I. Ahmed, M. Rehan, A. Basit, and K.-S. Hong, "Greenhouse gases emission reduction for electric power generation sector by efficient dispatching of thermal plants integrated with renewable systems," *Sci. Rep.*, vol. 12, no. 1, pp. 1–21, Jul. 2022, doi: 10.1038/s41598-022-15983-0.

[24] X. Lu, H. Li, K. Zhou, and S. Yang, "Optimal load dispatch of energy hub considering uncertainties of renewable energy and demand response," *Energy*, vol. 262, Jan. 2023, Art. no. 125564, doi: 10.1016/j.energy.2022.125564.

[25] I. Ahmed, A. Irshad, S. Zafar, B. A. Khan, M. Raza, and P. R. Ali, "The role of environmental initiatives and green value co-creation as mediators: Promoting corporate entrepreneurship and green innovation," *Social Netw. Bus. Econ.*, vol. 3, no. 4, pp. 1–22, Mar. 2023, doi: 10.1007/s43546-023-00465-w.

[26] U.-E.-H. Alvi, I. Ahmed, A. Alvi, B. Ashfaq, S. Mukhtar, and P. R. Ali, "Technological, financial and ecological analysis of photovoltaic power system using RETScreen: A case in Khuzdar, Pakistan," in *Proc. Int. Conf. Emerg. Technol. Electron., Comput. Commun. (ICETECC)*, Dec. 2022, pp. 1–6, doi: 10.1109/ICETECC56662.2022.10069314.

[27] A. H. Mirzahosseini and T. Taheri, "Environmental, technical and financial feasibility study of solar power plants by RETScreen, according to the targeting of energy subsidies in Iran," *Renew. Sustain. Energy Rev.*, vol. 16, no. 5, pp. 2806–2811, Jun. 2012, doi: 10.1016/j.rser.2012.01.066.

[28] C. S. Psomopoulos, G. C. Ioannidis, S. D. Kaminaris, K. D. Mardikis, and N. G. Katsikas, "A comparative evaluation of photovoltaic electricity production assessment software (PVGIS, PVWatts and RETScreen)," *Environ. Processes*, vol. 2, no. S1, pp. 175–189, Nov. 2015, doi: 10.1007/s40710-015-0092-4.

[29] I. Ahmed, U.-E.-H. Alvi, A. Basit, T. Khursheed, A. Alvi, K.-S. Hong, and M. Rehan, "A novel hybrid soft computing optimization framework for dynamic economic dispatch problem of complex non-convex contiguous constrained machines," *PLoS ONE*, vol. 17, no. 1, Jan. 2022, Art. no. e0261709, doi: 10.1371/journal.pone.0261709.

[30] I. Ahmed, M. Rehan, A. Basit, S. H. Malik, U.-E.-H. Alvi, and K.-S. Hong, "Multi-area economic emission dispatch for large-scale multi-fueled power plants contemplating inter-connected grid tie-lines power flow limitations," *Energy*, vol. 261, Dec. 2022, Art. no. 125178, doi: 10.1016/j.energy.2022.125178.

[31] M. Basu, "Multi-county combined heat and power dynamic economic emission dispatch incorporating electric vehicle parking lot," *Energy*, vol. 275, Jul. 2023, Art. no. 127523, doi: 10.1016/j.energy.2023.127523.

[32] M. Basu, "Multi-area dynamic economic emission dispatch of hydro-wind-thermal power system," *Renew. Energy Focus*, vol. 28, pp. 11–35, Mar. 2019, doi: 10.1016/j.ref.2018.09.007.

[33] I. Ahmed, M. Rehan, A. Basit, M. Tufail, and K.-S. Hong, "A dynamic optimal scheduling strategy for multi-charging scenarios of plug-in-electric vehicles over a smart grid," *IEEE Access*, vol. 11, pp. 28992–29008, 2023, doi: 10.1109/access.2023.3258859.

[34] F. A. T. Konchou, H. D. Temene, R. Tchinda, and D. Njomo, "Techno-economic and environmental design of an optimal hybrid energy system for a community multimedia centre in Cameroon," *Social Netw. Appl. Sci.*, vol. 3, no. 1, pp. 1–12, Jan. 2021, doi: 10.1007/s42452-021-04151-0.

[35] C. Ghenai, T. Salameh, and A. Merabet, "Technico-economic analysis of off grid solar PV/fuel cell energy system for residential community in desert region," *Int. J. Hydrogen Energy*, vol. 45, no. 20, pp. 11460–11470, Apr. 2020, doi: 10.1016/j.ijhydene.2018.05.110.

[36] Y. Chen, R. Wang, M. Ming, S. Cheng, Y. Bao, W. Zhang, and C. Zhang, "Constraint multi-objective optimal design of hybrid renewable energy system considering load characteristics," *Complex Intell. Syst.*, vol. 8, no. 2, pp. 803–817, Apr. 2022, doi: 10.1007/s40747-021-00363-4.

[37] M. F. Roslan, M. A. Hannan, P. J. Ker, R. A. Begum, T. I. Mahlia, and Z. Y. Dong, "Scheduling controller for microgrids energy management system using optimization algorithm in achieving cost saving and emission reduction," *Appl. Energy*, vol. 292, Jun. 2021, Art. no. 116883, doi: 10.1016/j.apenergy.2021.116883.

[38] S. Ahmadi and S. Abdi, "Application of the hybrid big bang–big crunch algorithm for optimal sizing of a stand-alone hybrid PV/wind/battery system," *Sol. Energy*, vol. 134, pp. 366–374, Sep. 2016, doi: 10.1016/j.solener.2016.05.019.

[39] A. M. Jasim, B. H. Jasim, F.-C. Baiceanu, and B.-C. Neagu, "Optimized sizing of energy management system for off-grid hybrid solar/wind/battery/biogasifier/diesel microgrid system," *Mathematics*, vol. 11, no. 5, p. 1248, Mar. 2023, doi: 10.3390/math11051248.

[40] A. F. Güven and M. M. Samy, "Performance analysis of autonomous green energy system based on multi and hybrid metaheuristic optimization approaches," *Energy Convers. Manage.*, vol. 269, Oct. 2022, Art. no. 116058, doi: 10.1016/j.enconman.2022.116058.

[41] A. Mahesh and K. S. Sandhu, "Optimal sizing of a grid-connected PV/wind/battery system using particle swarm optimization," *Iranian J. Sci. Technol., Trans. Electr. Eng.*, vol. 43, no. 1, pp. 107–121, Mar. 2019, doi: 10.1007/s40998-018-0083-3.

[42] M. M. Samy, M. I. Mosaad, and S. Barakat, "Optimal economic study of hybrid PV-wind-fuel cell system integrated to unreliable electric utility using hybrid search optimization technique," *Int. J. Hydrogen Energy*, vol. 46, no. 20, pp. 11217–11231, Mar. 2021, doi: 10.1016/j.ijhydene.2020.07.258.

[43] C. Parrado, A. Girard, F. Simon, and E. Fuentealba, "2050 LCOE (Levelized Cost of Energy) projection for a hybrid PV (photovoltaic)-CSP (concentrated solar power) plant in the Atacama Desert, Chile," *Energy*, vol. 94, pp. 422–430, Jan. 2016, doi: 10.1016/j.energy.2015.11.015.

[44] A. Maleki and F. Pourfayaz, "Optimal sizing of autonomous hybrid photovoltaic/wind/battery power system with LPSP technology by using evolutionary algorithms," *Sol. Energy*, vol. 115, pp. 471–483, May 2015, doi: 10.1016/j.solener.2015.03.004.

[45] E. L. V. Eriksson and E. M. Gray, "Optimization of renewable hybrid energy systems—A multi-objective approach," *Renew. Energy*, vol. 133, pp. 971–999, Apr. 2019, doi: 10.1016/j.renene.2018.10.053.

[46] I. B. Aydilek, "A hybrid firefly and particle swarm optimization algorithm for computationally expensive numerical problems," *Appl. Soft Comput. J.*, vol. 66, pp. 232–249, May 2018, doi: 10.1016/j.asoc.2018.02.025.

[47] P. Bajpai and V. Dash, "Hybrid renewable energy systems for power generation in stand-alone applications: A review," *Renew. Sustain. Energy Rev.*, vol. 16, no. 5, pp. 2926–2939, Jun. 2012, doi: 10.1016/j.rser.2012.02.009.

[48] L. El Boujdaini, A. Mezrhab, M. A. Moussaoui, F. Jurado, and D. Vera, "Sizing of a stand-alone PV–wind–battery–diesel hybrid energy system and optimal combination using a particle swarm optimization algorithm," *Electr. Eng.*, vol. 104, no. 5, pp. 3339–3359, Oct. 2022, doi: 10.1007/s00202-022-01529-0.

[49] X.-S. Yang, "Firefly algorithm, stochastic test functions and design optimization," *Int. J. Bio-Inspired Comput.*, vol. 2, no. 2, pp. 78–84, 2010, doi: 10.1504/IJBIC.2010.032124.

[50] T. Apostolopoulos and A. Vlachos, "Application of the firefly algorithm for solving the economic emissions load dispatch problem," *Int. J. Combinatorics*, vol. 2011, pp. 1–23, Dec. 2011, doi: 10.1155/2011/523806.

[51] A. H. Gandomi, X.-S. Yang, and A. H. Alavi, "Mixed variable structural optimization using firefly algorithm," *Comput. Struct.*, vol. 89, nos. 23–24, pp. 2325–2336, Dec. 2011, doi: 10.1016/j.compstruc.2011.08.002.

[52] Q. Changxing, B. Yiming, H. Huihua, and L. Yong, "A hybrid particle swarm optimization algorithm," in *Proc. 3rd IEEE Int. Conf. Comput. Commun. (ICCC)*, Dec. 2017, pp. 2187–2190, doi: 10.1109/CompComm.2017.8322924.

AYKUT FATİH GÜVEN was born in Tarsus, Turkey, in 1979. He received the B.S. and M.S. degrees in electrical engineering from Karadeniz Technical University, Trabzon, Turkey, in 2000 and 2004, respectively, and the Ph.D. degree in electrical engineering from the Department of Electrical Engineering, Kocaeli University, Kocaeli, Turkey, in 2022. He is currently a Doctoral Researcher with the Department of Energy Systems Engineering, Faculty of Engineering, Yalova University, Yalova, Turkey. His research interests include renewable energy, hybrid energy systems management, power system analysis, meta-heuristic optimization, and deep learning.

NURAN YÖRÜKEREN received the B.S. and M.S. degrees in electrical engineering from Yıldız Technical University, Istanbul, Turkey, in 1985 and 1989, respectively, and the Ph.D. degree in electrical engineering from the Department of Electrical Engineering, Kocaeli University, Kocaeli, Turkey, in 1994. She became an Assistant Professor, in 1994, and a Professor, in 2021, with Kocaeli University, where she is currently the Deputy Head of the Department of the Electrical Engineering. Her research interests include power system analysis, generating stations and plants, electric power transmission, renewable energy, power system harmonics, and transmission line mechanic design.

ELSAYED TAG-ELDIN is currently with the Faculty of Engineering and Technology, Future University in Egypt, on leave from Cairo University after nearly 30 years of service with the Faculty of Engineering. He was the Dean of the Faculty of Engineering, Cairo University, where he achieved many unique signs of progress in both academia and research on the impact of emerging technologies in electrical engineering. He was a PI of several nationally and internationally funded projects. He has many publications in highly refereed international journals and specialized conferences in the applications of artificial intelligence on protection of electrical power networks. In addition, he is on the editorial boards of several international journals.

MOHAMED MAHMOUD SAMY received the B.Sc. degree in electrical engineering from the Faculty of Engineering and Technology, Banha University, Banha, Egypt, in 1995, the M.Sc. degree in electrical power and machines from Zagazig University, Zagazig, Egypt, in 2007, and the Ph.D. degree from Cairo University, Giza, Egypt, in 2011.

He is currently a Professor with the Department of Electrical Engineering, Faculty of Engineering, Beni-Suef University, Beni-Suef, Egypt.

Prof. Samy was awarded the prize of the Best Ph.D. Thesis in electrical engineering from the Faculty of Engineering, Cairo University, in 2012. He was elected as a Technical Program Committee (TPC) Member for the Third International Conference on Energy Engineering and Environmental Protection (EEEP2018).